

MEASUREMENT OF HEAT TRANSFER COEFFICIENT IN
CONCENTRIC AND ECCENTRIC ANNULI

by

WASIUDDIN CHOUDHURY

B.Sc.Eng., University of Dacca, 1958

A THESIS SUBMITTED IN PARTIAL FULFILMENT OF
THE REQUIREMENTS FOR THE DEGREE OF

MASTER OF APPLIED SCIENCE

in the Department

of

Mechanical Engineering

We accept this thesis as conforming to the
required standard

THE UNIVERSITY OF BRITISH COLUMBIA

APRIL, 1963

In presenting this thesis in partial fulfilment of the requirements for an advanced degree at the University of British Columbia, I agree that the Library shall make it freely available for reference and study. I further agree that permission for extensive copying of this thesis for scholarly purposes may be granted by the Head of my Department or by his representatives. It is understood that copying or publications of this thesis for financial gain shall not be allowed without my written permission.

Department of Mechanical Engineering,
The University of British Columbia,
Vancouver 8, Canada.

April, 1963.

ABSTRACT

Heat transfer coefficients were measured at the inner wall of smooth concentric and eccentric annuli. The annuli were formed by an outer plastic tube of 3 in. inside diameter and an inner core cylinder of 1 in. outside diameter. Air at room temperature was allowed to flow through the annuli at a Reynolds number range from 15,000 to 65,000.

The measurement of heat transfer coefficient was made by a transient heat transfer test technique. The method consisted in establishing an initial temperature gradient between the fluid and a solid body mounted on the core cylinder by heating, then observing and recording the temperature-time history of the body as it returned to equilibrium condition with the fluid stream. The heat transfer coefficient was calculated from this record.

The final results were presented in graphical form showing variations of Nusselt number with Reynolds number. The results of the concentric annulus tests agreed favourably with those predicted by Wiegand (2) and Monrad and Pelton (3). The effect of eccentricity was to reduce the heat transfer coefficient although the general trend was identical to that in the concentric annulus case.

It was observed that the decrease of heat transfer coefficient was not linearly related to the eccentricity of the core cylinder. The effect of eccentricity was more pronounced in the range $0 \leq e \leq 0.5$ where the value of heat transfer coefficient decreased considerably.

ACKNOWLEDGEMENT

The author would like to thank the many persons whose direct or indirect assistance has made this report possible. He should like to mention some of them by name:

Professor W. O. Richmond deserves many thanks for his continued encouragement and assistance during all phases of the work.

Professors V. J. Modi, N. Epstein, C. A. Brockely and Mr. J. D. Denton for many valuable discussions during different phases of the project.

Professor W. A. Wolfe who suggested the present topic and through whose initial efforts the project was started.

Finally the author would like to express his thanks for the permission to use the Computing Centre at the University of British Columbia and the National Research Council of Canada for providing funds to make this research possible.

TABLE OF CONTENTS

	Page
CHAPTER I	
Introduction	1
Definitions of Terms Used	2
Review of Literature on Annuli	3
CHAPTER II	
The Transient Test Technique	9
Discussion of Assumptions	12
CHAPTER III	
Apparatus	15
Instrumentation	24
CHAPTER IV	
Experimental Procedure	27
Presentation of Results	28
Discussion of Results	34
CHAPTER V	
Conclusions	44
Recommendations	45
BIBLIOGRAPHY	46
APPENDIX I	
Air Metering System	49

Page

APPENDIX II

Physical Properties and Constants of the Thermal Capacitors	52
--	----

APPENDIX III

Physical Properties of Air	53
--------------------------------------	----

APPENDIX IV

Sample Calculations	56
-------------------------------	----

APPENDIX V

Tables of Experimental Results	57
--	----

LIST OF FIGURES

	Page
1. Schematic Layout of the Concentric Annulus Tests . . .	19
2. Test Models and Mounting Structures	20
3. Schematic Layout of the Eccentric Annulus Tests . . .	21
4. Method of Supporting Inner Tube	22
5. Photographs of Test Section and Capacitors	23
6. Thermocouple Circuit	26
7. A Typical Temperature-Time Relation as Obtained on the Recorder	29
8. Heat Transfer at Inner Wall of Annulus, $e = 0$	30
9. Heat Transfer at Inner Wall of Annulus, $e = 0.25$	31
10. Heat Transfer at Inner Wall of Annulus, $e = 0.50$	32
11. Heat Transfer at Inner Wall of Annulus, $e = 1.0$	33
12. Variation of Nusselt Number with Reynolds Number and Eccentricity Parameter	35
13. Variation of Heat Transfer Coefficient with Inner Tube Eccentricity	36
14. Comparison of Heat Transfer Data Obtained by Capacitors No. 1 and No. 2	38
15. A Typical Semi-Log Plot of Dimensionless Temperature with Time	41
16. Thermocouple Locations in the Capacitor	42
17. Dynamic Viscosity of Air at Atmospheric Pressure	54
18. Thermal Conductivity of Air at Atmospheric Pressure . . .	55

LIST OF TABLES

	Page
I. Details of Orifice	51
II. Properties of Thermal Capacitors	52
III. Biot Number of the Capacitors	52
IV. Temperature-Time Data for Capacitor No. 1, $e = 0$. .	58
V. Data for Computing Reynolds and Nusselt Numbers for Capacitor No. 1, $e = 0$	59
VI. Temperature-Time Data for Capacitor No. 1, $e = 0.25$.	60
VII. Data for Computing Reynolds and Nusselt Numbers for Capacitor No. 1, $e = 0.25$	61
VIII. Temperature-Time Data for Capacitor No. 1, $e = 0.50$.	62
IX. Data for Computing Reynolds and Nusselt Numbers for Capacitor No. 1, $e = 0.50$	63
X. Temperature-Time Data for Capacitor No. 1, $e = 1.0$. .	64
XI. Data for Computing Reynolds and Nusselt Numbers for Capacitor No. 1, $e = 1.0$	65
XII. Temperature-Time Data for Capacitor No. 2, $e = 0$. .	66
XIII. Data for Computing Reynolds and Nusselt Numbers for Capacitor No. 2, $e = 0$	67

LIST OF SYMBOLS

a, a^1	- constants
A	- surface area of the capacitor, ft^2
C	- heat capacity of the capacitor, $\text{Btu}/^\circ\text{F}$
C_p	- specific heat of air, $\text{Btu}/\text{lb. } ^\circ\text{F}$
C_p^1	- specific heat of the capacitor, $\text{Btu}/\text{lb } ^\circ\text{F}$
C_1	- heat capacity of the supporting plastic, $\text{Btu}/^\circ\text{F}$
D_1	- outer diameter of the inner cylinder, ft
D_2	- inner diameter of the outer tube, ft
D_e	- hydraulic equivalent diameter, $\frac{4 \times \text{flow area}}{\text{wetted perimeter}}$, ft
D_n	- Nusselt equivalent diameter, $\frac{4 \times \text{flow area}}{\text{heated perimeter}}$, ft
e	- eccentricity parameter
G	- mass velocity, $\text{lb}/\text{hr ft}^2$
h	- average heat transfer coefficient, $\text{Btu}/\text{hr ft}^2 ^\circ\text{F}$
h_m	- maximum velocity head, in. of water
h_s	- static pressure head, in. of water
h_w	- pressure drop across orifice, in. of water
K	- thermal conductivity of fluid, $\text{Btu}/\text{hr ft } ^\circ\text{F}$
K_1	- thermal conductivity of plastic support, $\text{Btu}/\text{hr ft } ^\circ\text{F}$
K_s	- thermal conductivity of capacitor material, $\text{Btu}/\text{hr ft } ^\circ\text{F}$
m, m^1	- constants
n, n^1	- constants
N_{Nu}	- Nusselt number, $\frac{hD_e}{K}$

N_{Pr}	- Prandtl number, $\frac{\mu C_p}{K}$
N_{Re}	- Reynolds number, $\frac{GD_e}{\mu}$
r_1	- outer radius of the inner cylinder, ft
r_2	- inner radius of the outer tube, ft
r_m	- radius at the point of maximum velocity, ft
T	- temperature of the capacitor at any instant, chart div.
T_a	- temperature of air, chart div. or F
T_o	- temperature of capacitor at zero time, chart div.
T^*	- dimensionless temperature
V_{avg}	- average flow velocity, ft/hr
V_{max}	- maximum point velocity, ft/hr
w	- mass of the capacitor, lb
θ	- time, sec
λ	- slope, 1/hr
μ	- dynamic viscosity of air, lb/hr ft
μ_w	- dynamic viscosity of air at the solid wall, lb/hr ft
ρ	- density of air, lb/ft ³
τ_c	- time constant of the capacitor, sec
τ_i	- time constant of the instrument, sec
ϕ_1, ϕ_2	- functions

CHAPTER I

INTRODUCTION

The purpose of this investigation was to measure the heat transfer coefficients in an annulus formed by placing a smooth cylinder at various positions inside a circular tube with fluid flowing turbulently along the longitudinal axis of the cylinder. The heat flow was through the inner cylinder surface and the variations of heat transfer coefficients due to different positions of the inner cylinder were studied. The investigation was limited to the Reynolds number range from 15,000 to 65,000.

This problem is of interest because of developments in the peaceful uses of atomic energy which necessitates a knowledge of heat transfer coefficients in certain types of odd-shaped flow passages. In the present designs of heat exchangers and nuclear reactors, the coolant flows in longitudinal passages formed by the spaces between parallel rods or tubes in closely spaced arrays within a cylindrical container. In gas cooled nuclear reactors, arrays of fuel bearing rods are cooled by gas flowing parallel to the longitudinal axes of the rods. This general configuration provides increased heat transfer surface to compensate for the reduced heat transfer coefficients associated with gaseous flows. This type of flow geometry has received very little attention from research workers. This has resulted in the use of heat transfer coefficients in design which are not always safe and accurate. An experimental programme was undertaken for the very simplest case of this geometry, namely an annular cross-section.

The usual method of determining the heat transfer coefficients requires the measurement of the temperature of the heat transfer medium and of the heat transfer surface under steady-state conditions. It is difficult to measure the surface temperature accurately so that steady-state methods require elaborate apparatus and instrumentation. To obviate these difficulties a non-stationary method has been used in this investigation. This method, the transient heat transfer test technique (1)* is based on the cooling of a body having fixed thermophysical properties under a step-change of temperature. The underlying theory of this technique will be discussed in detail in the next chapter.

Using this technique results were obtained for heat transfer in the concentric annulus. These results were compared with correlations given by Wiegand (2) and Monrad and Pelton (3). Results for the eccentric annulus were also obtained in a similar manner. These latter results are of interest because of the paucity of data for the eccentric annulus.

DEFINITIONS OF TERMS USED

Annulus An annulus is defined as the flow passage formed by placing a cylindrical core inside a circular tube with fluid flowing along the longitudinal axis of the core. When the cylindrical core is at the centre of the outer tube the resulting flow cross-section is termed a concentric annulus. An eccentric annulus is formed by placing the core cylinder at positions other than the centre of the outer tube.

* Numbers in parentheses refer to bibliography at the end of the Thesis.

Thermal Capacitor The heated solid body used in the experiment is called the thermal capacitor cylinder. For the sake of brevity in the subsequent chapters this will be called the capacitor.

REVIEW OF LITERATURE ON ANNULI

Concentric Annulus A large number of experiments has been carried out on heat transfer in turbulent flow in a concentric annulus. Most investigators attacked the problem by dimensional analysis and presented equation basically of the form,

$$N_{Nu} = a (N_{Re})^m (N_{Pr})^n \phi_1 \left(\frac{D_2}{D_1} \right) \text{-----} [1]$$

where, N_{Nu} = Nusselt number, $\frac{hD_e}{K}$

N_{Re} = Reynolds number, $\frac{GD_e}{\mu}$

N_{Pr} = Prandtl number, $\frac{\mu C_p}{K}$

a, m and n are constants which were determined experimentally.

This equation is of the same form as that for conduit flow,

$$N_{Nu} = a^1 (N_{Re})^{m^1} (N_{Pr})^{n^1}, \text{ with the addition of the term, } \phi_1 \left(\frac{D_2}{D_1} \right)$$

to include the dimensional characteristic of the annulus.

Jordan (24), in 1909, studied the heat transfer from the inner wall of two vertical annuli of different dimensions. The annuli were formed by placing a copper pipe inside a cast iron casing. The diameter ratios were 1.25 and 1.47. Air at temperatures varying from 240 F to 700 F was passed through the inner tube and water at

temperatures up to 200 F was circulated through the annular space. The test section was 40 ft. long and it was placed directly after an elbow. The experimental results covered a Reynolds number range from 7,000 to 95,000.

Thompson and Foust (25), in 1940, investigated the heat transfer characteristics in two double-pipe heat exchangers. One of them was made of one inch pyrex tubing jacketed with two inch iron pipe; the other was two inch pyrex tubing in a three inch pipe. Cold water at 50 F to 95 F flowed through the annular space and steam was condensed at the inner pyrex tube. The test section was 10 ft. long and was placed directly after an elbow. The heat transfer coefficient was determined from the overall resistance by assuming that the coefficient was a function of water velocity in the annulus only. The experimental data was taken at Reynolds number greater than 100,000.

Foust and Christian (4), in the same year, investigated the heat transfer coefficients in annuli having various thicknesses of the annular passage. The annulus was formed by assembling thin walled copper tubing inside standard iron pipe. The diameter ratio ranged from 1.20 to 2.56. Water flowed through the annular space and steam was condensed inside the copper tube. The test section was 8.66 ft. long with no provision for a calming section. The heat transfer coefficient was calculated by graphical differentiation. The investigation covered a Reynolds number range from 3,000 to 60,000. The equation recommended was,

$$\frac{hD_n}{K} = 0.04 \left(\frac{GD_n}{\mu} \right)^{0.8} \left(\frac{\mu C_p}{K} \right)^{0.4} \left(\frac{D_2}{D_1} \right) \text{-----} [2]$$

This equation was based on Nusselt's equivalent diameter, D_n defined as,

$$D_n = \frac{4 \times \text{Flow area}}{\text{Heated Perimeter}}$$

The authors also found that the results could be correlated by using the conventional equivalent diameter, based on the wetted perimeter, by the following equation,

$$\frac{hD_e}{K} = 0.032 \left(\frac{GD_e}{\mu} \right)^{0.8} \left(\frac{\mu C_p}{K} \right)^{0.4} \left(\frac{D_2}{D_1} \right) \text{-----} [3]$$

Zebran (26) in the same year also studied the heat transfer characteristics at the inner wall of an annulus. The core cylinder was electrically heated and air was forced through the annular passage. Five different diameter ratios were used ranging from 1.18 to 2.72. Provisions were made for a calming section which varied between 8 and 125 equivalent diameters. The heat transfer coefficients were calculated by measuring the core wall temperature and the temperature of the air stream. The experimental data covered the Reynolds number range from 2,600 to 120,000.

Monrad and Pelton (3) in the same year presented experimental results of heat transfer coefficients in three different annuli with two different fluids flowing in turbulent flow. The diameter ratios were 1.65, 2.45 and 17 for heat transfer from inner wall, and 1.85 for heat transfer from outer wall. The test section was 6.5 ft. long with a calming section at the entrance. The investigation covered a Reynolds number range from 12,000 to 220,000. The experimental data

for heat transfer at the inner wall were correlated by the equation,

$$\frac{hD_e}{K} = 0.02 \left(\frac{GD_e}{\mu} \right)^{0.8} \cdot \left(\frac{\mu G_p}{K} \right)^n \left(\frac{D_2}{D_1} \right)^{0.53} \quad [4]$$

where $n = 0.4$ for heating and 0.3 for cooling. The properties were evaluated at the main stream temperature. It was also suggested, on the assumption that the relative skin friction on the two surfaces was the same for turbulent as for laminar flow, that the constant term,

$$0.02 \left(\frac{D_2}{D_1} \right)^{0.53}, \text{ in equation [4] could be modified for better accuracy to } 0.023 \left(\frac{2 \ln D_2/D_1 - (D_2/D_1)^2 + 1}{D_2/D_1 - D_1/D_2 - 2(D_2/D_1) \ln D_2/D_1} \right).$$

It is to be noted here that the agreement between the equations of Foust and Christian, and Monrad and Pelton is very poor. As Barrow (5) pointed out, for diameter ratios 16 and 2.4 respectively, the former investigators predict results 6.0 times and 2.2 times greater than those predicted by the latter investigators.

Mueller (6), also in the same year, investigated heat transfer from a fine wire placed inside a tube. This was a very special case of annuli because with such a small core and large thickness of annulus a combination of cross flow and parallel flow is likely to exist. Therefore, his correlations could not be compared with an annulus of the proportion used in this investigation.

Davis (7), in 1943, presented another equation for heat transfer from inner wall with turbulent flow of fluids. The equation was

obtained by dimensional analysis and was valid for diameter ratios from 1.18 to 6,800. The suggested equation was,

$$\frac{hD_1}{K} = 0.031 \left(\frac{GD_1}{\mu} \right)^{0.8} \left(\frac{\mu C_p}{K} \right)^{1/3} \left(\frac{\mu}{\mu_w} \right)^{0.14} \left(\frac{D_2}{D_1} \right)^{0.15} \quad [5]$$

The constants in this equation were determined by comparison with the experimental data of other investigators.

McMillen and Larson (27), in 1944, obtained annular heat transfer coefficients in a double pipe heat exchanger. The test section consisted of four passes having different annular spaces with brass or steel tube placed inside a standard iron pipe. The diameter ratios were 1.245, 1.3, 1.532 and 1.970. The length of the test section was 11 ft. There were no calming sections at the entrance of each pass. The coefficients were calculated by assuming that all the thermal resistances except that of the film were constant. The experimental data covered a Reynolds number range from 10,000 to 100,000. The best correlation of data was given by the equation,

$$\left(\frac{h}{C_p G} \right) \left(N_{Re} \right)^{0.2} \left(N_{Pr} \right)^{2/3} = 0.0305 \quad \text{-----} \quad [6]$$

Wiegand (2), in 1945, made a detailed study of all the experimental data on heat transfer from the inner wall. The best correlation fitting these data was found to be,

$$\frac{hD_e}{K} = 0.023 \left(\frac{GD_e}{\mu} \right)^{0.8} \left(\frac{\mu C_p}{K} \right)^{1/3} \left(\frac{D_2}{D_1} \right)^{0.45} \quad \text{----} \quad [7]$$

The equation was valid for Reynolds number greater than 10,000 where the properties were calculated at the bulk temperature.

Apart from dimensional analysis, this problem has also been attempted by establishing an analogy between fluid friction and heat transfer. In 1951, Mizushima (10) investigated this approach but the analysis was quite difficult due to lack of similarity between the velocity and temperature profiles when heat was flowing from the inner wall only. Using many assumptions Mizushima derived an equation for the heat transfer coefficient which was very complicated for general use. Barrow (11), in 1961, presented a semi-theoretical solution by considering the transfer of heat and transfer of momentum. The solution was applicable for fluids having a Prandtl number equal to unity.

Eccentric Annulus Heat transfer in eccentric annuli has received very little attention. Deissler and Taylor (12), in 1955, made a theoretical analysis of fully developed turbulent heat transfer in an eccentric annulus. It was found that the average Nusselt number decreased as the eccentricity of the inner tube was increased. It was also shown that the Nusselt numbers for a concentric annulus were slightly higher than those for a tube with an equivalent diameter.

In 1962, Leung, Kays and Reynolds (13) presented heat transfer data in concentric and eccentric annuli based on a theoretical study as well as an experimental investigation. For the eccentric annulus the diameter ratios ranged from 2.0 to 3.92 and for the concentric annulus from 2.0 to 5.2. Air was flowing through the annulus under fully developed turbulent flow conditions. The experimental results covered a Reynolds number range from 10,000 to 150,000.

CHAPTER II

THE TRANSIENT TEST TECHNIQUE

The transient heat transfer test technique as used in this investigation has also been used by other investigators in different types of flow situations. London, Boelter and Nottage (1) proposed this method in 1941, Eber (14) used this method to obtain data on heat transfer characteristics in supersonic flow over cones, and Fischer and Norris (15) determined the convective heat transfer coefficient by an analysis of skin temperature measurements on the nose of a V-2 rocket in flight. In the past decade Garbett (16) used the transient technique to determine the heat transfer coefficient from bodies in high velocity flow. Kays, London and Lo (17) demonstrated successfully its usefulness in determining the heat transfer coefficient for gas flows normal to tube banks.

Basically the transient technique for determining heat transfer coefficient consists in establishing an initial temperature potential between the fluid and the body by heating or cooling, then observing and recording the temperature-time history of the body as it returns towards equilibrium with the fluid stream. The heat transfer coefficient is calculated from this record.

The simplest case of transient heating or cooling of a body is one in which the internal resistance of the body is negligibly small in comparison with the thermal resistance of the solid-fluid interface. This is because such a system permits the lumping of all the resistances to heat transfer at the boundary of the solid body.

This idealisation is based on the assumption that the material of the capacitor has infinitely large thermal conductivity. Many transient heat flow problems can be solved with reasonable accuracy by assuming that the internal conductive resistance is so small that the temperature throughout the body is uniform at any instant of time.

A quantitative measure of the relative importance of the two resistances can be expressed by a dimensionless modulus, called the Biot number, which is defined as,

$$N_{Bi} = \frac{h\bar{L}}{K_s}$$

where, h = surface coefficient of heat transfer

\bar{L} = a characteristic length, $\frac{\text{Volume of the body}}{\text{Surface area}}$

K_s = thermal conductivity of the body

As Kreith (18) pointed out, for bodies whose shape resembles a plate, a cylinder, or a sphere, the error introduced by assuming that the internal temperature at any instant is uniform will be less than 5 per cent when the internal resistance is less than 10 per cent of the external surface resistance. In other words this will hold when $N_{Bi} \leq 0.1$.

Keeping in mind the above requirement, the capacitor of the present experiment was made of copper which has one of the highest thermal conductivities amongst the naturally available metals. For a capacitor of this metal, the rate of temperature change will depend

only on the average surface heat transfer coefficient which varies mainly with the fluid properties, the flow conditions, and the flow geometry.

The theoretical equation describing the energy balance on the cooling capacitor under this idealised condition can be formulated as,

$$\left[\begin{array}{l} \text{The change of internal energy} \\ \text{of the thermal capacitor dur-} \\ \text{ing a small interval of time} \end{array} \right] = \left[\begin{array}{l} \text{The net heat flow from} \\ \text{the thermal capacitor to} \\ \text{the fluid stream during} \\ \text{the same interval of time} \end{array} \right]$$

$$-C \, dT = hA (T - T_a) \, d\theta \quad \text{-----} \quad [8]$$

where, C = heat capacity of the capacitor

A = surface area in contact with fluid stream

θ = time

T = temperature of the cooling capacitor at any θ

T_a = temperature of the fluid stream

The minus sign on the left hand side in equation [8] indicates that the internal energy decreased when $T > T_a$ as was the case in this experiment.

In solving equation [8], C , A and T_a are assumed constant.

For small variation of T and constant flow, h will be essentially constant. The solution becomes,

$$\frac{T - T_a}{T_o - T_a} = \exp \left(- \frac{hA}{C} \right) \theta \quad \text{-----} \quad [9]$$

where, T_o = temperature of the capacitor at $\theta = 0$.

This equation can be rewritten in the following form,

$$\log_e T^* = \left(-\frac{hA}{C} \right) \theta \quad \text{-----} \quad [10]$$

$$\text{where, } T^* = \frac{T - T_a}{T_o - T_a}$$

If the assumption is legitimate then a plot of $\log_e T^*$ as the ordinate and θ as the abscissa would yield a straight line the slope of which will be $-\left(\frac{hA}{C}\right)$. From this slope the value of h can be calculated.

DISCUSSION OF ASSUMPTIONS

In establishing and solving equation [8] several assumptions have been made. A critical evaluation of these assumptions is necessary at this stage to support the applicability of the transient test technique to heat transfer in annular flow.

1. The assumption involving the idealisation that all resistances to heat transfer are lumped at the solid fluid interface is the key point to the whole analysis. Accuracy requirements for a given problem determine whether or not this approach is useful. In most heat transfer experiments, results with an error of plus or minus 25 per cent may be considered very good. However, Kays, London and Lo (17) claimed that their experimental error was plus or minus 5 per cent where they used a similar method for the cross-flow heat exchanger. It is expected that in the present experiment the error would be confined to the same limit.

2. Heat transfer is assumed to be by forced convection only.

In a fully developed turbulent flow free convection effects are almost negligible. However, in viscous flow with a large annular gap the possibility of free convection effects cannot be totally ignored. In this experiment the flow conditions were always turbulent and therefore free convection effects can be neglected.

It is also assumed that radiation effects are negligible.

For small temperature difference at low temperature level with polished model surfaces this effect would be very small. But for high temperatures, radiation loss can be significant which means that the heat transfer coefficient as determined by this method would contain a contribution from the radiation coefficient. Temperatures of about 60 to 70 F above ambient can be considered low enough so as not to cause any serious error due to radiation. The present experiment was conducted in this range of temperature.

3. The temperature difference in the radial direction inside the capacitor and in the axial direction along its length is negligible. This can be achieved by having a thermal capacitor of very high thermal conductivity and relatively thin wall thickness.

4. Heat loss to the supporting structure of the model is assumed very small. As Garbett (16) noted in his investigation, the mounting structure sometimes provide additional sources of heat loss. For example, during a cooling process the capacitor cools much faster than the supporting medium so that towards the end of the transient cooling heat may flow from the supports to the capacitor. This effect

can be best reduced by keeping the area of contact between capacitor and support small and using supporting material having a small $(K_1 C_1)$ product,

where, K_1 = thermal conductivity of the supporting material
 C_1 = heat capacity of the supporting material

5. The average value of the specific heat of the material of the capacitor is constant. The specific heat of copper is essentially constant between temperatures 70 to 150 F. The mass of the capacitor is also constant and therefore the heat capacity is constant.

6. The bulk temperature of the fluid stream is constant during the test. To verify this air temperature was measured continuously at the outlet of the test section for the duration of one complete run. It was found that the variation was not more than 1 F which was less than 1.5 per cent of the ambient temperature.

CHAPTER III

APPARATUS

The apparatus was designed to measure the following:

- (a) the air flow rate
- (b) the temperature and pressure of air
- (c) the temperature-time history of the capacitor

Two different arrangements of apparatus were used. One for the study of the concentric annulus and another for the eccentric annulus. In Figure 1, a schematic layout of the apparatus used for the concentric annulus is shown. The arrangement consisted of a test section, a mixing box and a centrifugal blower. The test section, shown in Figure 2, was made of transparent plastic outer tube having an inside diameter, $D_2 = 3$ in., and a wall thickness of $1/4$ in. The inner cylinder on which the capacitor was mounted had an outside diameter, $D_1 = 1$ in.

Air at room temperature was blown through the test section by a $1/3$ hp centrifugal type blower with a speed rating of 3450 rpm. The air flow rate was determined by measuring the maximum velocity in the annulus by a pitot static tube placed at the downstream end of the test section and connected to a micro-manometer.

A mixing box between the blower and the test section acted as a surge tank and tended to smooth pulsations in the air stream.

The temperature variation of the cooling capacitor was measured by a copper-constantan thermocouple connected to an automatic recorder to obtain a temperature-time history.

The apparatus used for the eccentric annulus test is shown schematically in Figure 3. The same test section and mixing box were used in this arrangement but a higher capacity blower was used to allow an orifice meter to be used for measuring air flow. In the eccentric annulus the air flow rate could not be determined by pitot tube as in the case of concentric annulus because of the non-symmetrical form of velocity profile in an eccentric annulus. The flow rate was therefore measured by a flat plate, square edged orifice placed upstream of the test section. The large pressure drop across the orifice required the higher capacity blower to cover the same range of Reynolds number as was obtained in the concentric annulus flow. A detailed description of the two air metering systems is given in Appendix I.

The blower used in the second arrangement was a $3\frac{1}{4}$ hp centrifugal type blower with a speed rating of 3450 rpm. Air temperature was measured by a mercury in glass thermometer graduated to 1 F and also by a copper-constantan thermocouple placed in the mixing box. The change in the flow Reynolds number was accomplished by throttling the air flow at the inlet side of the fan.

The length of the test section was selected to give a fully developed hydrodynamic flow. There is still a considerable doubt as to the exact length after which the flow is fully established in an annulus. One group of investigators, Miller, Byrnes and Benforado (19)

claimed that in a concentric annulus the velocity profile is established in twenty equivalent diameters. In the present investigation, this figure was taken as the design criterion to select the length of the test section. It was also found that there was no reliable information available as to the entry length required for the establishment of a fully developed flow in an eccentric annulus. However, it was assumed that the entry length in both concentric and eccentric annuli was of the same order of magnitude.

The heat transfer characteristics of the capacitor was studied by recording its temperature-time history during a transient cooling period. Two capacitors were used. The first one, shown in Figure 2, was 2.125 in. long with an outside diameter of 1 in. and an inside diameter of 0.776 in. The capacitor was made from solid copper rod drilled to the required inside diameter and faced to the desired length. A small hole was drilled in the wall of the capacitor to provide space for the thermocouple junction. In selecting the size of the capacitor, care was taken to comply with the Biot number requirements and other assumptions made in Chapter II.

A second capacitor was made of the same material as the first but was smaller in length and mass. It was 1.4703 in. long with an outside diameter of 1 in. and an inside diameter of 0.7175 in. Figure 2 shows the dimensions of this capacitor. A few tests were made with this capacitor to show that the length of the capacitors had little effect on the results obtained. Further details of the comparison are given in Chapter IV.

The capacitor was mounted in the test section at the downstream end of the inner cylinder. The mounting structure consisted of two plastic end pieces, one on each side of the capacitor. The plastic sections had the same outside diameter as the capacitor so that final assembled form has a smooth outside surface. For the concentric annulus the remaining length of the inner cylinder, upstream of the capacitor, consisted of a solid plastic rod having an outside diameter of 1 in. Any small deflection due to the weight of the rod could be ignored considering the large thickness of the annular passage. But in the eccentric annulus, especially when the inner cylinder was closer to the wall of the outer tube, any small deflection would cause distortion in the flow pattern. To minimise this effect the inner cylinder was made of thin walled aluminium tubing with plastic end pieces to allow for the mounting of the capacitor. The overall deflection of the aluminum tube was less than 0.010 in.

Supports at the two ends were used to position the inner cylinder within the tube. To align the tube accurately templates were made from aluminium plate. These templates had an outside diameter of 3 in. with an one inch hole made at the required eccentricities, namely, $e = 0$, $e = 0.25$ and $e = 0.50$. Having aligned the cylinder with these templates, two thin metallic spiders crossing at right angles were placed at the two ends of the cylinder. Right angled grooves were made at both ends of the inner cylinder to locate the spiders. The inner cylinder with the spiders was then easily slid into the outer tube. The same procedure was followed for the eccentric annulus but in this case the line of intersection of the two spiders

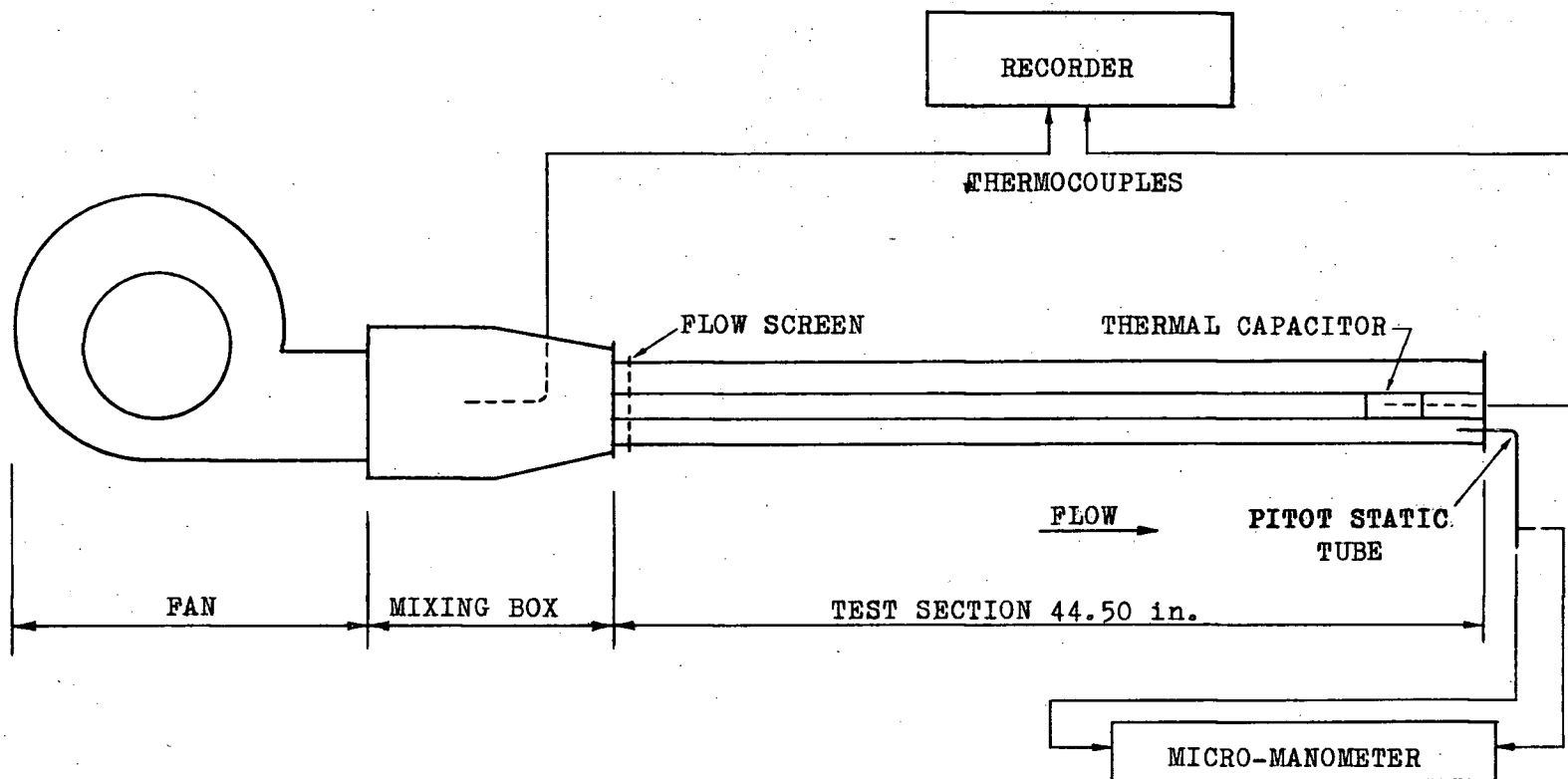
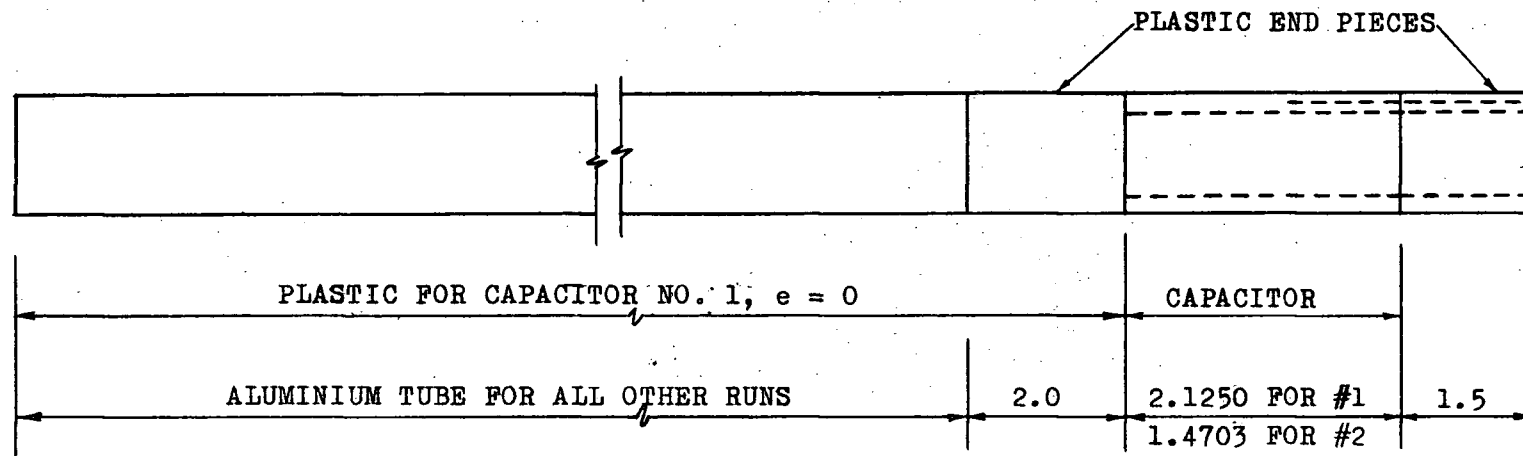
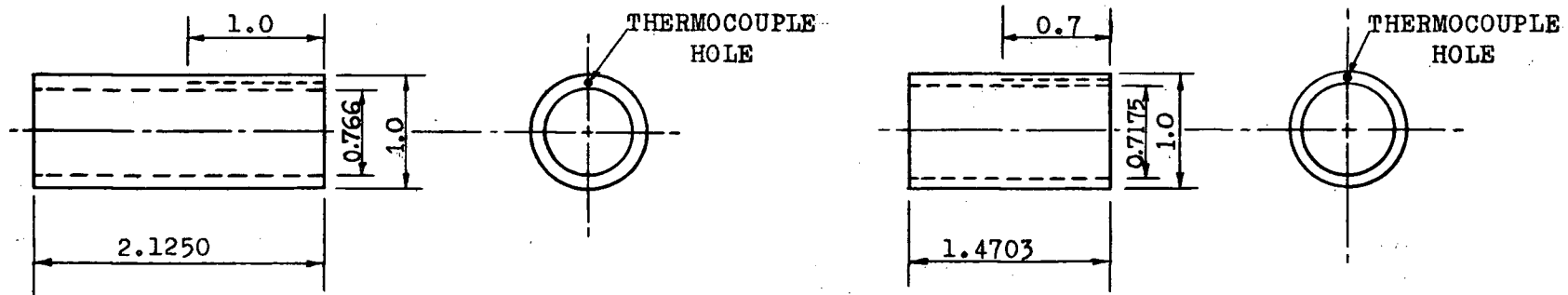


FIG. 1. SCHEMATIC LAYOUT OF THE CONCENTRIC ANNULUS TESTS



SUPPORTING ROD FOR CAPACITORS



CAPACITOR NO. 1

CAPACITOR NO. 2

NOTE: ALL DIMENSIONS IN INCHES

FIG. 2. TEST MODELS AND MOUNTING STRUCTURES

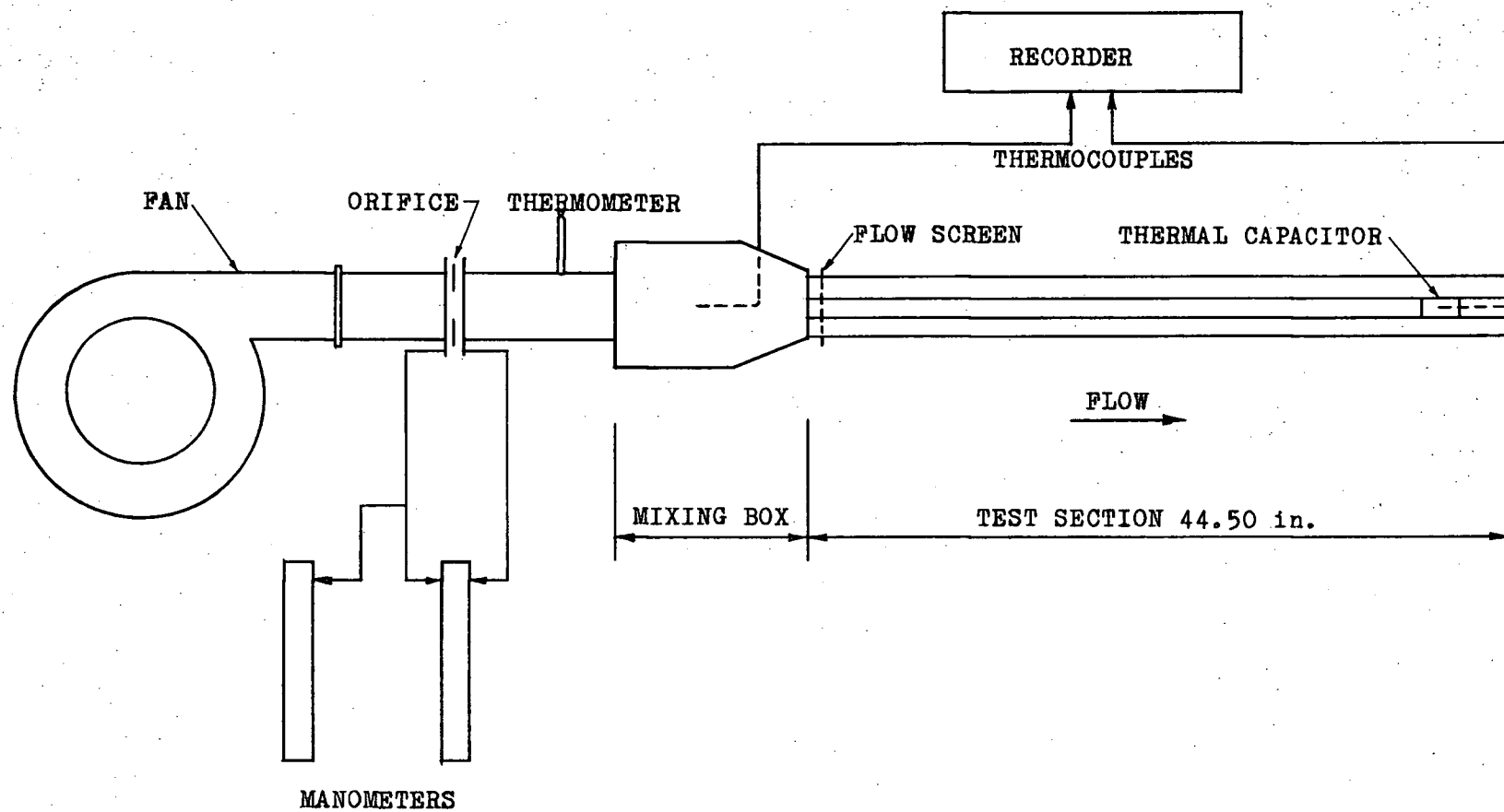
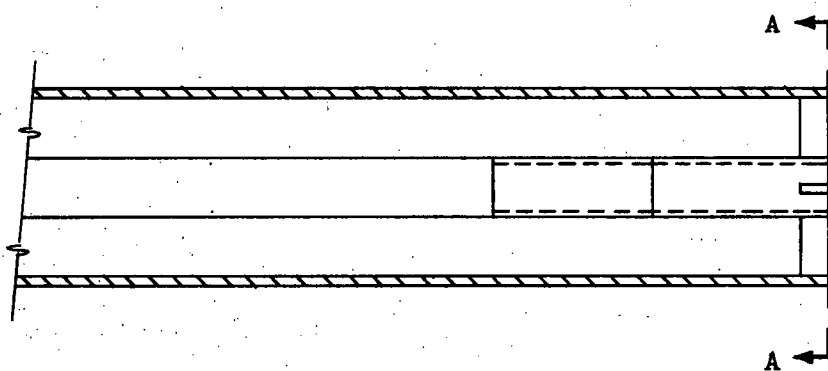
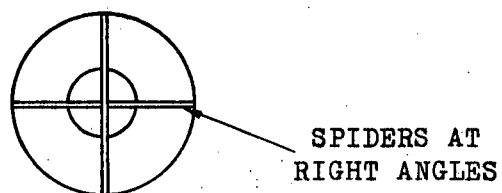


FIG. 3. SCHEMATIC LAYOUT OF THE ECCENTRIC ANNULUS TESTS

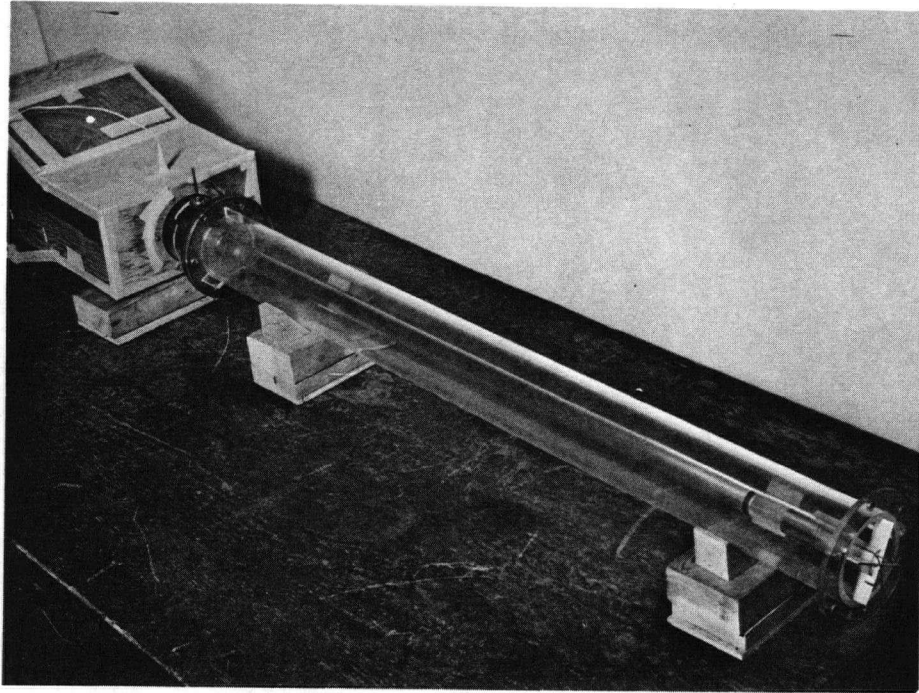


TEST SECTION SHOWING SUPPORT AT ONE END.
OTHER END SIMILAR

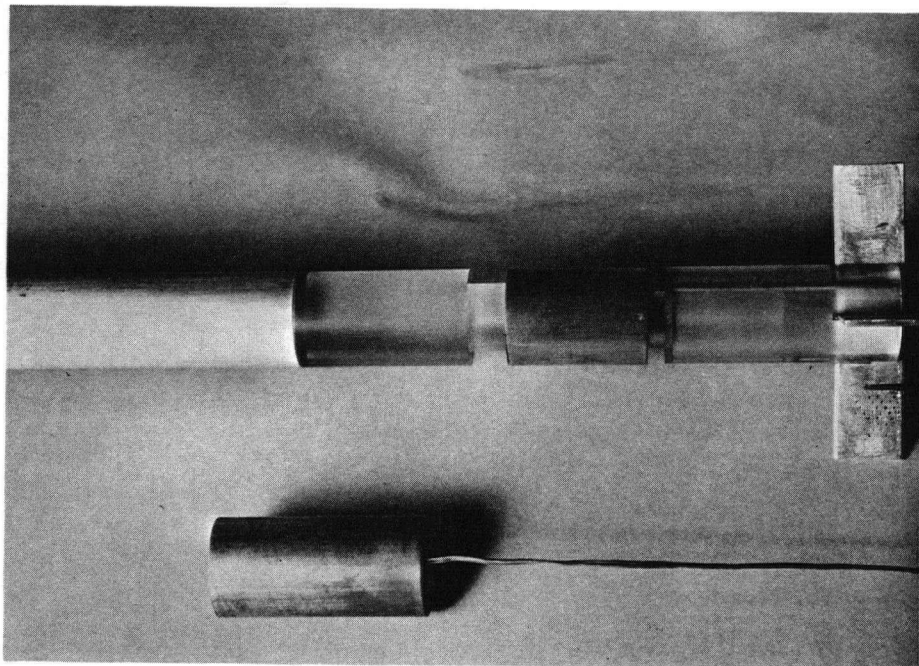


SECTION A-A

FIG. 4. METHOD OF SUPPORTING INNER TUBE FOR $e = 0$



(a) PHOTOGRAPH OF TEST SECTION



(b) PHOTOGRAPH OF CAPACITORS

FIG. 5. PHOTOGRAPHS OF TEST SECTION AND CAPACITORS

was shifted to give the desired eccentricity of the inner cylinder. The supporting device for the concentric annulus is shown in Figure 4. Photographs of the test section and the capacitors are shown in Figure 5.

INSTRUMENTATION

As mentioned in the earlier chapter, the heat transfer coefficient was determined from a record of the temperature-time history of the cooling capacitor. Since the temperature of the capacitor was decreasing with time, a measuring probe capable of fast response to a changing temperature was desired. An ideal temperature measuring probe would faithfully respond to any change regardless of the time rate of temperature change of the capacitor. The thermocouple was the obvious choice for this type of measurement because of the following reasons:

The time constant of the thermocouple wire is a function of the ratio of heat capacity to its surface area. The thermocouple junctions have small mass and hence small thermal capacity. The area of contact is comparatively large due to soldering of the probe to the capacitor. Therefore, the thermocouple wire has a small time constant and follows closely any temperature variation in the capacitor.

In the range of the experiment, which was from 70 to 140 F, the electro-motive force of the thermocouple is practically a linear function of the temperature. Thus it was possible to plot the dimensionless temperature T^* in equation [10] in terms of the emf difference

instead of the temperature difference. This simplified not only the computation but also the calibration of the recording instrument.

The copper-constantan thermocouple used for measuring the capacitor temperature and the air temperature in the mixing box was 26 gauge B & S, solid wire with polyvinyl insulation.

The temperature-time variation of the capacitor was recorded on the chart of a Bristol recorder. The range of the recorder was adjusted to 0 to 2.5 millivolts and the chart speed was kept constant at $3/8$ in. per min. It was believed that the Bristol recorder had a faster response than that of the capacitor so any error due to instrument lag was negligible. A quantitative estimate of the relative error will be presented in the discussion of results, Chapter IV. This error, according to Garbett (16), is the ratio of the instrument time constant to the capacitor time constant.

Two thermocouples were used in the experimental arrangement with a selector switch to connect one thermocouple to the recorder at any one time. A schematic diagram of the thermocouple circuit with related instrumentation is shown in Figure 6.

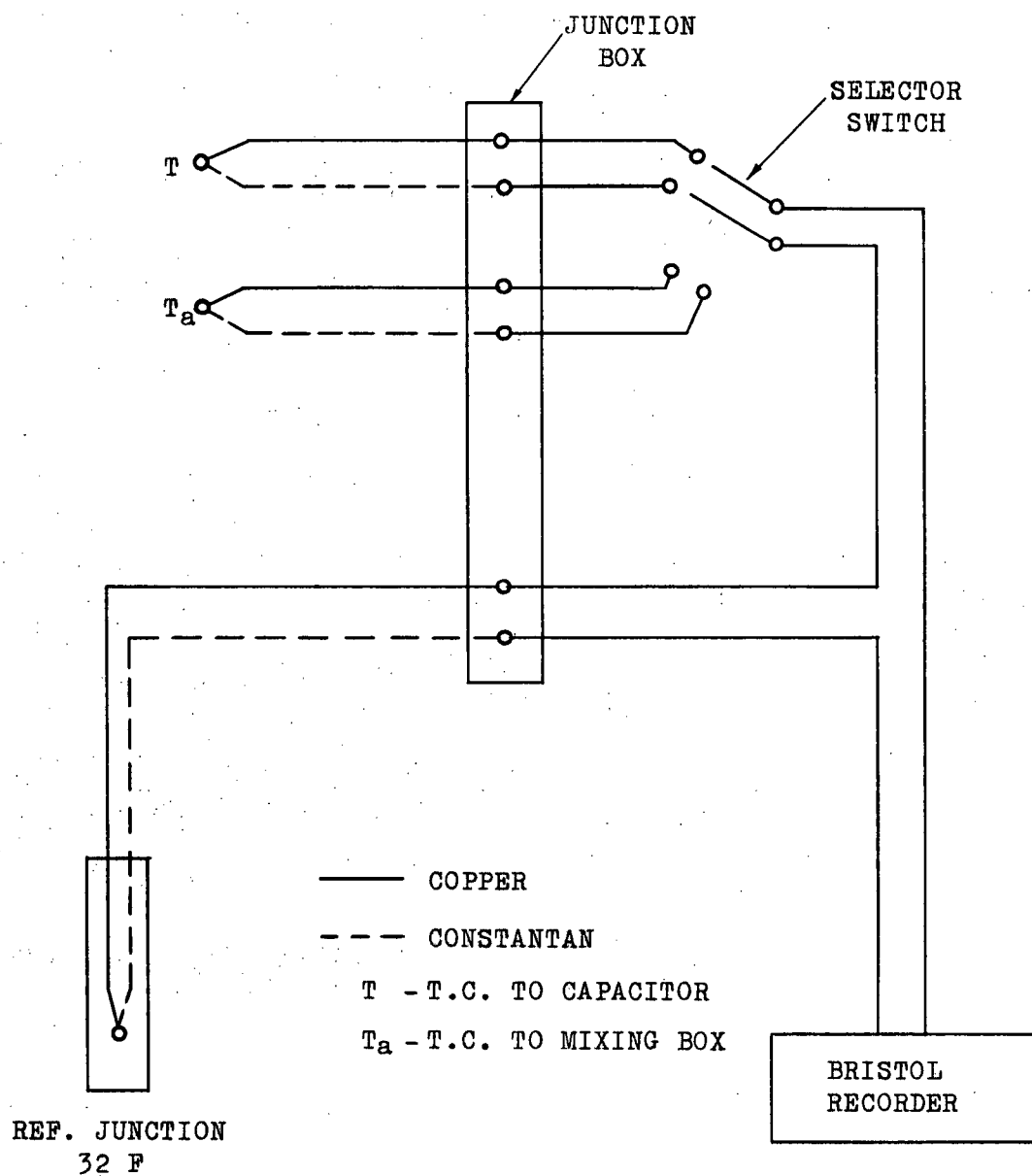


FIG. 6. THERMOCOUPLE CIRCUIT

CHAPTER IV

EXPERIMENTAL PROCEDURE

For each set of experiments the inner tube was first aligned to the particular eccentricity for which the test was to be made. The capacitor was then heated to 60 to 70 F above the ambient temperature by an external heat source consisting of an electric soldering iron with an aluminium extension piece to reach the capacitor inside the tube. The heat source was then withdrawn, the recorder and the air fan motor switch were turned on. As the capacitor was cooling towards equilibrium in the fluid stream, a continuous record of temperature against time was made in the recorder. This record was taken for approximately 130 seconds. The selector switch was then turned on to the air temperature thermocouple and a record of this temperature was also made on the same chart. About the middle of each run orifice pressure drop, static pressure and temperature of air at the inlet side of the orifice and the air velocity were recorded. When one test was complete, the flow rate was changed by throttling the air at the inlet to the fan. The same procedure was then repeated till a Reynolds number range from 15,000 to 65,000 was covered. A total of about 13 to 16 runs were taken for each position of the annulus.

Four positions of the annulus were investigated. Each position was designated by the eccentricity parameter, e , defined by the following relation:

$$e = \frac{\text{Distance between the centres of the two cylinders}}{r_2 - r_1}$$

The four positions were thus, $e = 0$, $e = 0.25$, $e = 0.50$, and $e = 1.0$.

PRESENTATION OF RESULTS

The temperature time history of the capacitor as obtained for a typical run is shown in Figure 7. For the purposes of computation all the experimental data were entered in tables given in Appendix V. The final results have been presented in graphical form with dimensionless parameters on log-log co-ordinates. This presentation was of the following form:

$$N_{Nu} = \phi_2(N_{Re})$$

In the present experiment, the air was at room temperature which at times varied between 70 F and 90 F. The Prandtl number for air in this temperature range is practically constant. Therefore, a log-log plot of Nusselt numbers as a function of Reynolds numbers only have been presented.

In Figure 8, the variation of Nusselt number with Reynolds number has been shown for an annulus with eccentricity parameter equal to zero. In the same sheet equations of other investigators such as Wiegand (2), Monrad and Pelton (3) and Foust and Christian (4) have also been plotted.

The results of the eccentric annulus for three different eccentricity parameters, $e = 0.25$, $e = 0.50$ and $e = 1.0$ are shown in Figures 9, 10 and 11 respectively. In each case, the best line correlating the data is also shown.

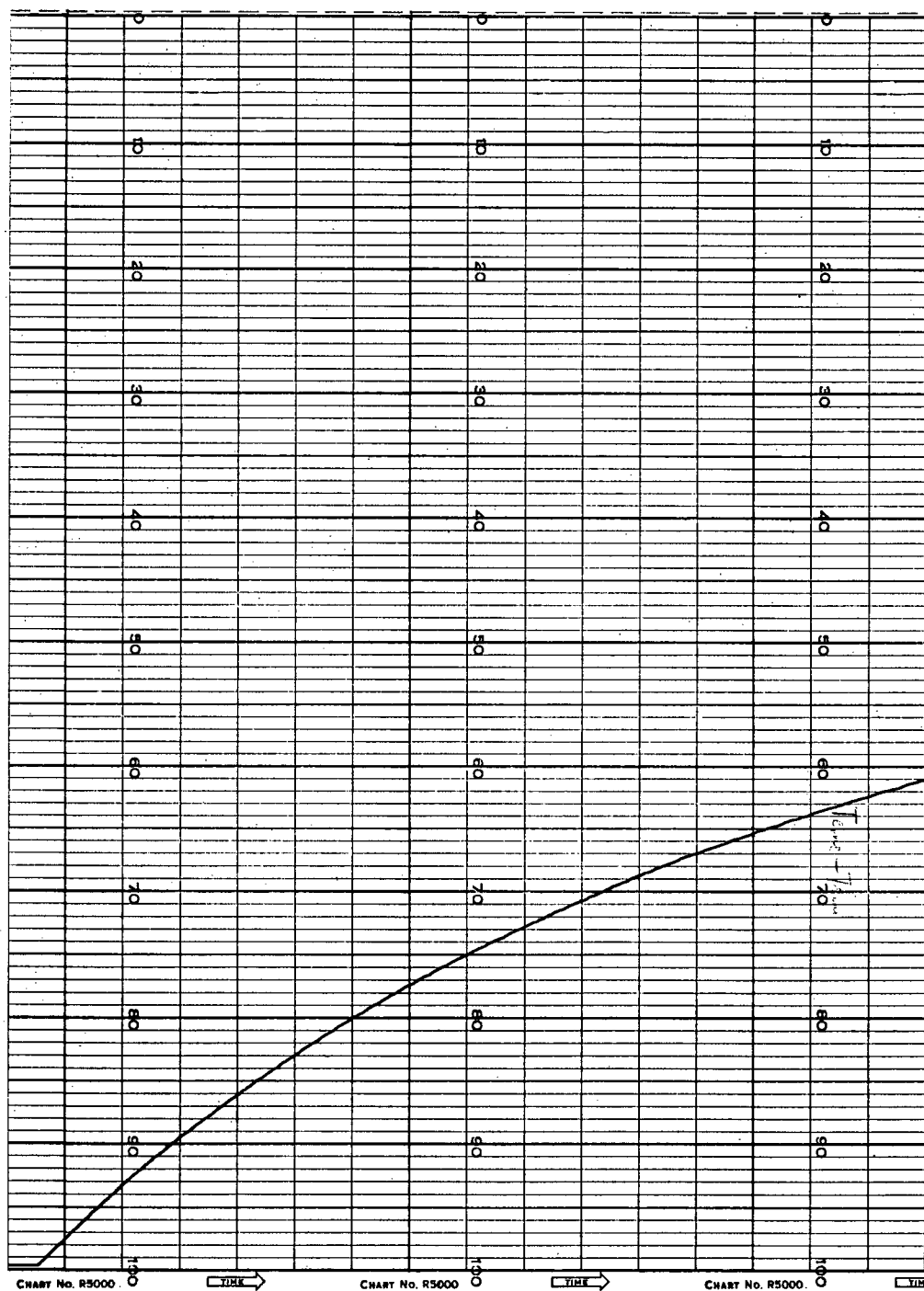


FIG. 7. A TYPICAL TEMPERATURE-TIME RELATION AS OBTAINED ON THE RECORDER

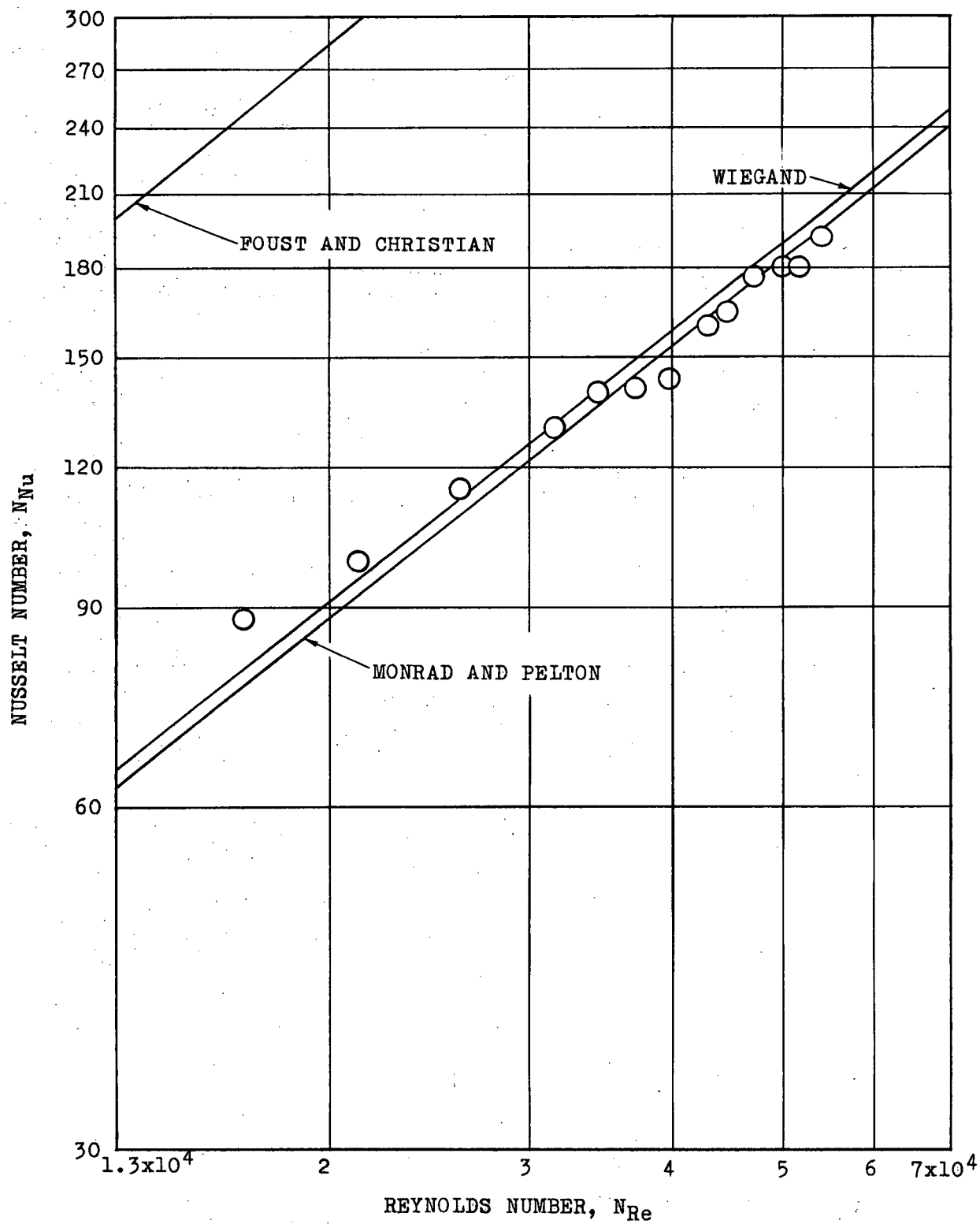


FIG. 8. HEAT TRANSFER AT INNER WALL OF ANNULUS, $e = 0$

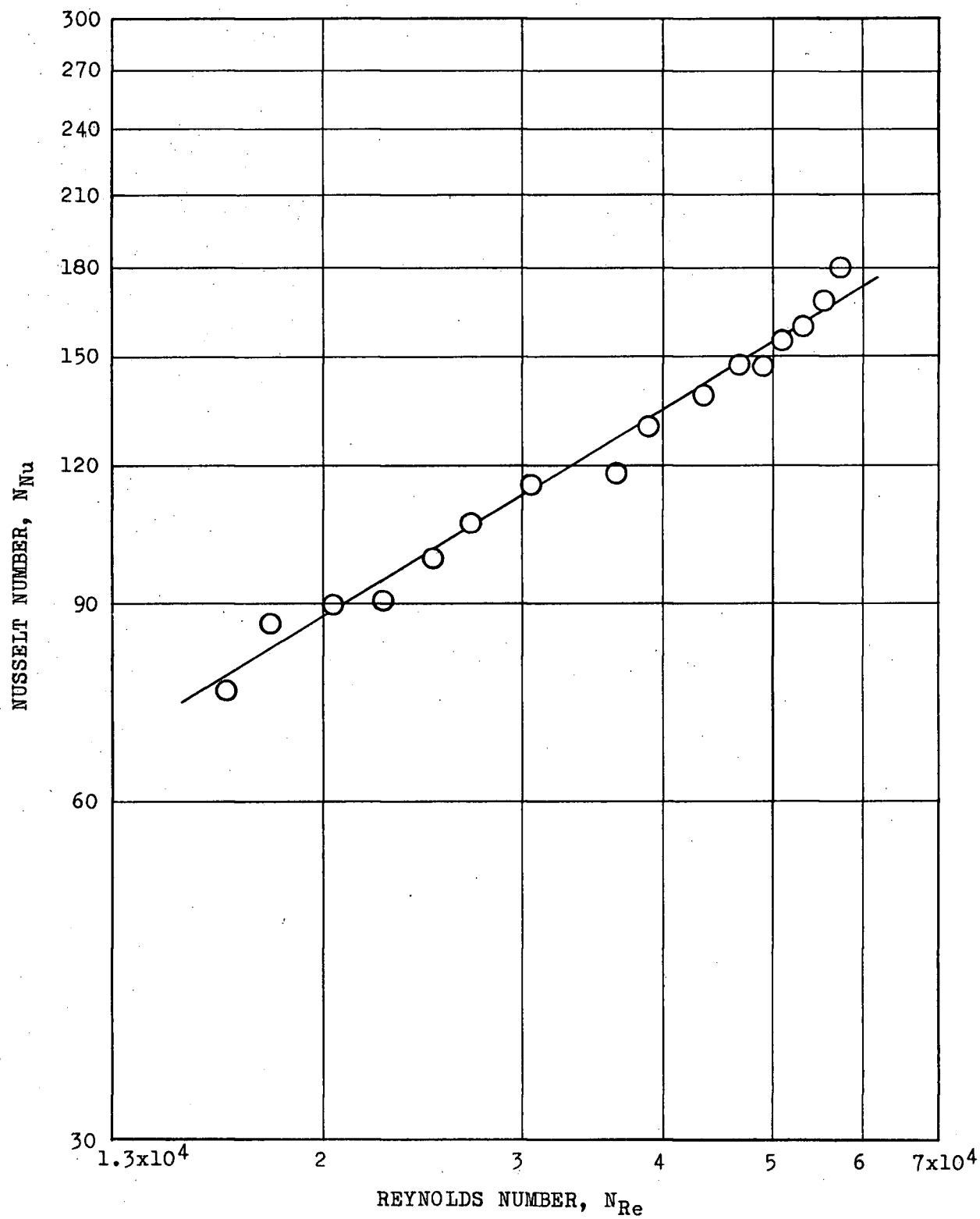


FIG. 9. HEAT TRANSFER AT INNER WALL OF ANNULUS, $e = 0.25$

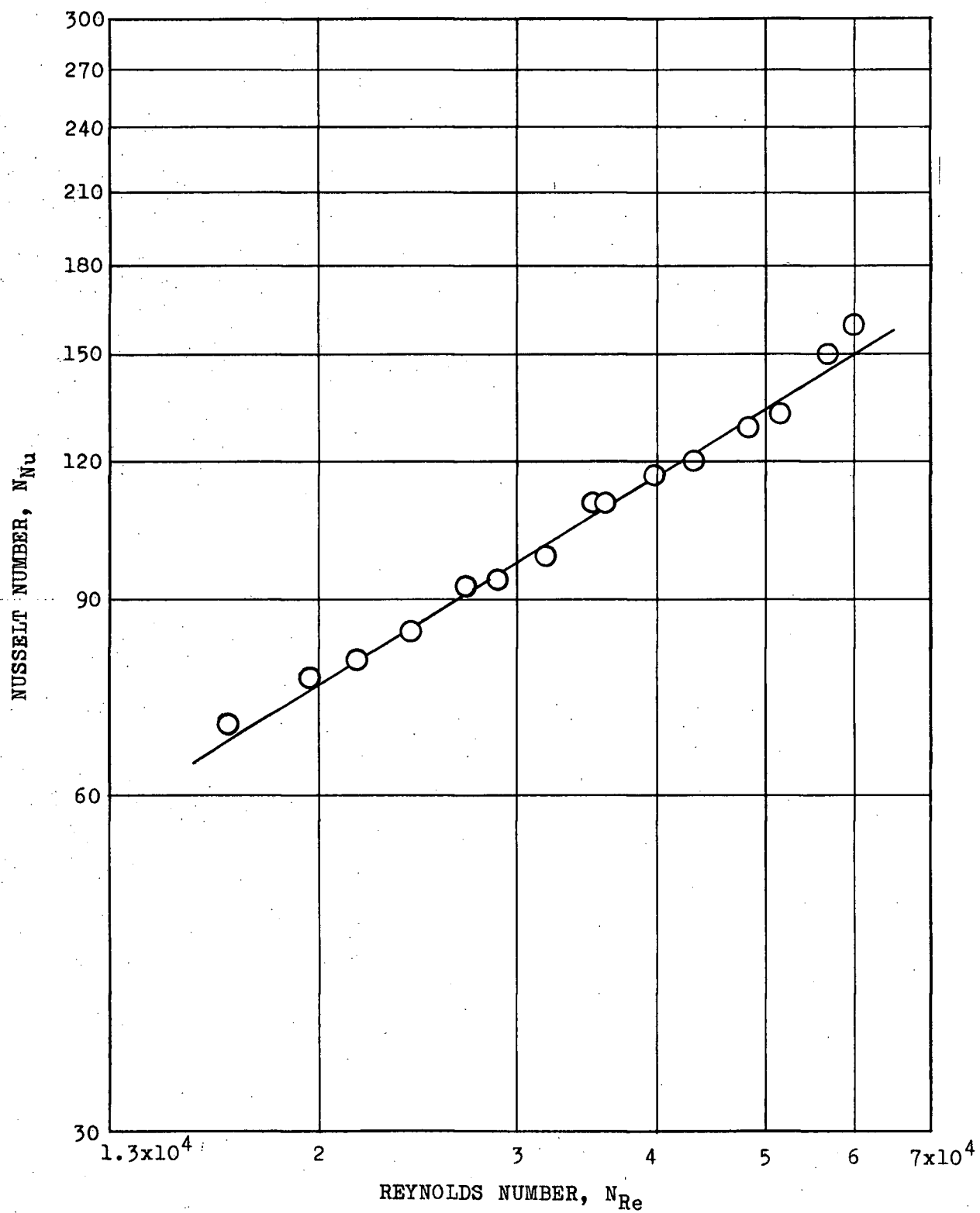


FIG. 10. HEAT TRANSFER AT INNER WALL OF ANNULUS, $e = 0.50$

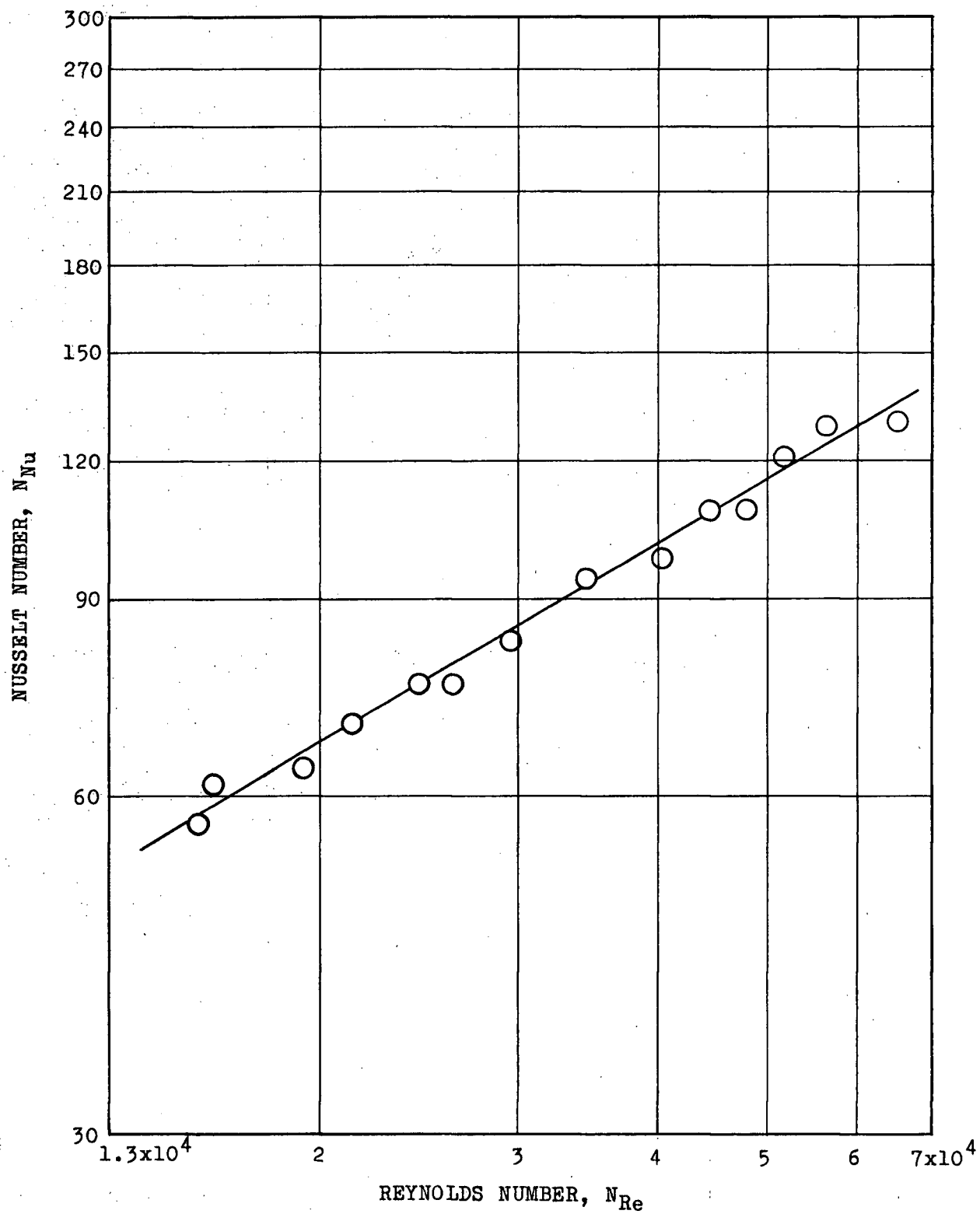


FIG. 11. HEAT TRANSFER AT INNER WALL OF ANNULUS, $e = 1.0$

In Figure 12, the variation of Nusselt number with Reynolds number and eccentricity parameter is shown. It is interesting to note that the average Nusselt number decreased with increasing annulus eccentricity. In Figure 13, this decreasing trend of Nusselt number with eccentricity parameter has been plotted for a fixed Reynolds number.

DISCUSSION OF RESULTS

This section includes a discussion of all the experimental results and an evaluation of the probable errors involved in different parts of the investigation.

Experimental data for the average heat transfer coefficient in a concentric annulus are shown in Figure 8. Since all these data were obtained in almost isothermal condition, the Prandtl number of the air was always constant. The equations [7] of Wiegand, [4] of Monrad and Pelton and [3] of Foust and Christian are plotted in the same sheet to compare the experimental results. It is noted that the agreement is very good indeed with equations [7] and [4]. The equation of Foust and Christian predicts much higher values of heat transfer coefficients although the trend shown is the same. Foust and Christian obtained their water side coefficients by means of a semi-graphical method which resulted in steam coefficients which were very high so that their results have been questioned by latter investigators (5, 21).

The equation [5] of Davis (7) was not considered a proper comparison with the present data because it is based on the inside

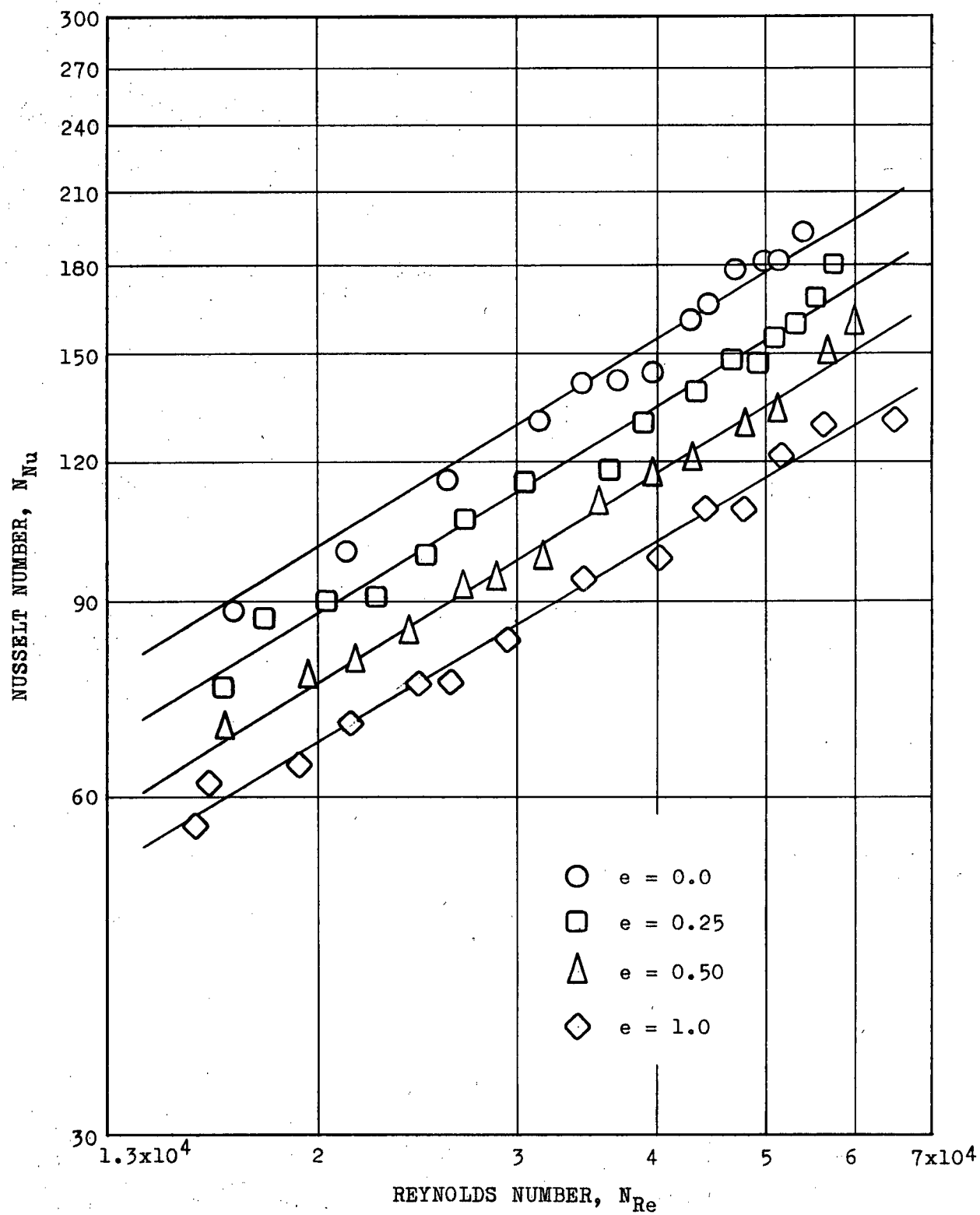


FIG. 12. VARIATION OF NUSSELT NUMBER WITH REYNOLDS NUMBER AND ECCENTRICITY PARAMETER

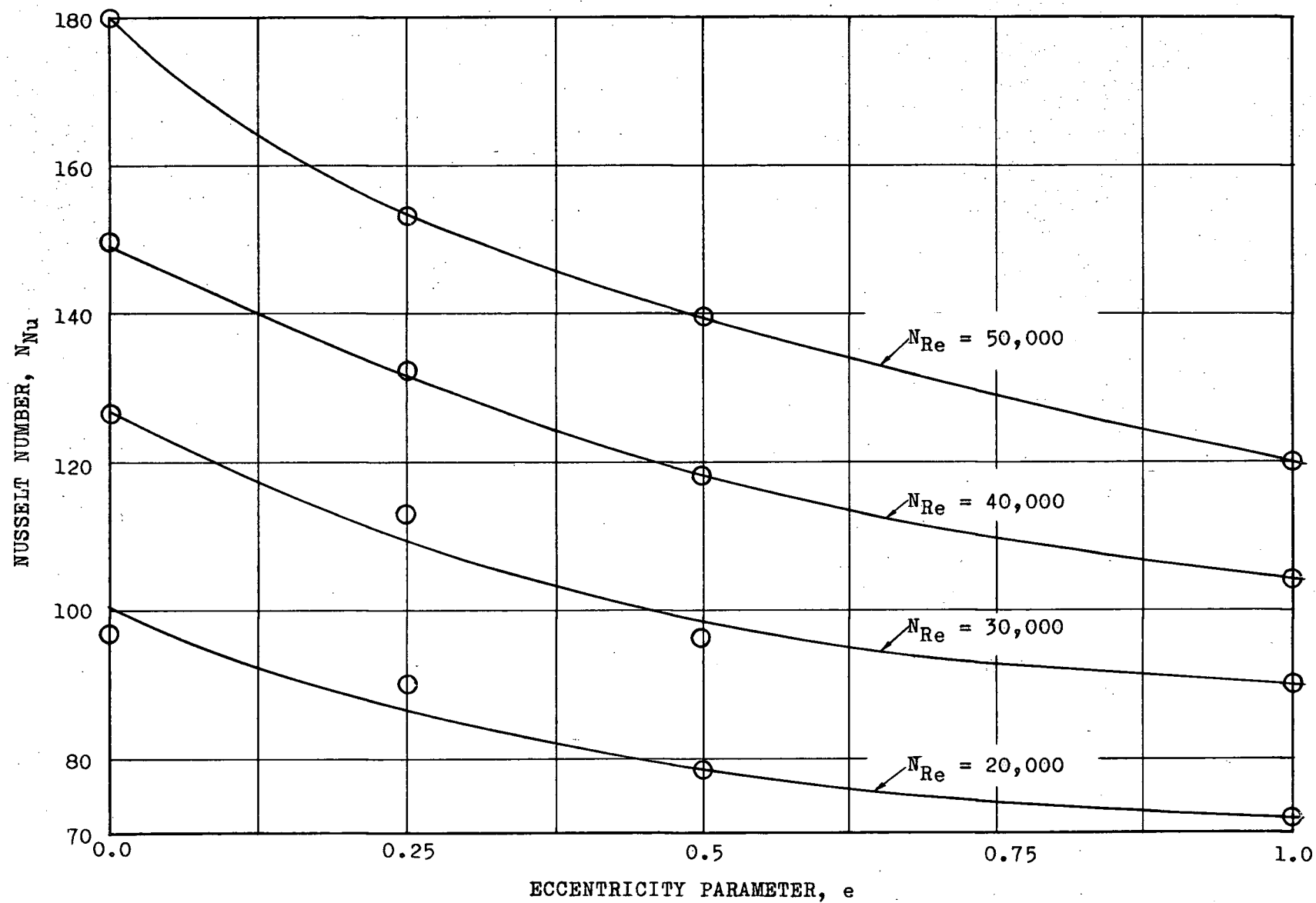


FIG. 13. VARIATION OF HEAT TRANSFER COEFFICIENT WITH INNER TUBE ECCENTRICITY

diameter of the annulus. Davis agreed that when heat transfer occurred only at the inner surface the use of inside diameter in the Nusselt and Reynolds numbers was reasonable. However, as Barrow (5) pointed out the computation of Reynolds number based on the inside wall diameter can in no way be considered as a measure of the kind of flow. Also the friction in annuli results from resistance at both the inner and outer wall of the annulus. Therefore, the most reasonable definition of Reynolds number is the one based on the conventional equivalent diameter, D_e .

The heat transfer coefficients presented here are claimed to be the average value in a fully developed turbulent flow. A question may arise as to the validity of this statement on the grounds that the thermal boundary layer was not completely developed in the length of the capacitor. As mentioned in Chapter II the transient technique does measure the average heat transfer coefficient, provided all assumptions have been satisfied. To justify this statement a second experiment was carried out for the same annulus but with a capacitor of different length. Capacitor No. 2 was thus designed with a length of 1.4703 in. thereby having a reduction in length of 30 per cent of that of Capacitor No. 1. Figure 2 shows the details of the second capacitor. The heat transfer data obtained by using both these capacitors are plotted in Figure 14. The good agreement between these results indicates that the earlier statement was reasonable.

Kays, London and Lo (17) pointed out that the transient technique is not adequate for laminar flow because of the tendency

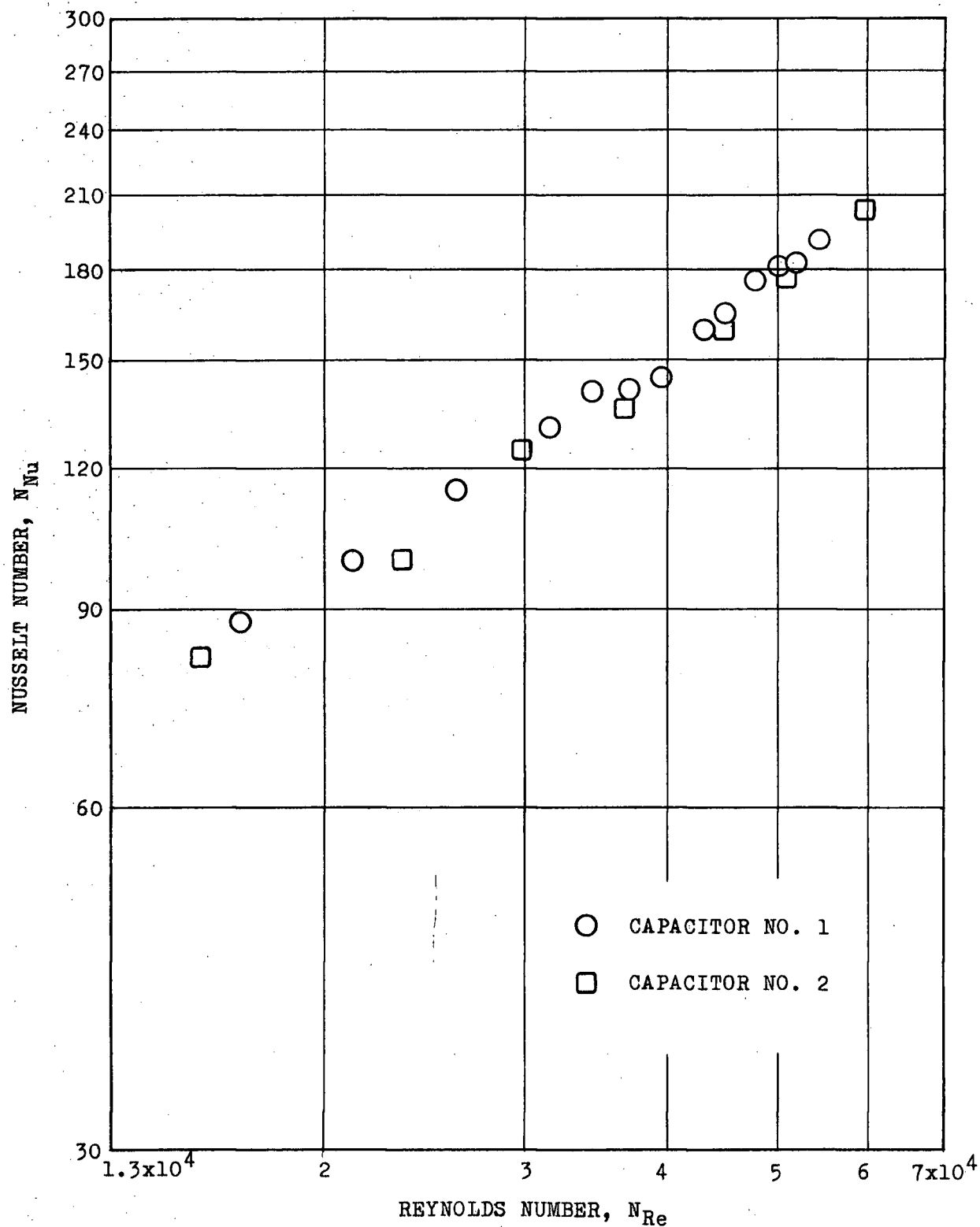


FIG. 14. COMPARISON OF HEAT TRANSFER DATA OBTAINED BY CAPACITORS NO. 1 AND NO. 2

of the temperature profile to extend completely across the flow stream rather than being confined to a relatively thin boundary layer such as in turbulent flow. This is why the transient technique gives the average values of heat transfer coefficients provided the flow is fully turbulent. In addition, the results shown in Figure 8 also suggest that the data obtained in this investigation are the average heat transfer coefficients.

Referring to Figure 8 again, it may be noted that the experimental point at the lowest Reynolds number tends to be higher than that predicted by the equations of Weigand and Monrad and Pelton. It is believed that at very low Reynolds number the cooling rate of the capacitor becomes very slow and hence towards the end of the cooling period the capacitor is likely to lose heat to the surrounding supports at each end. At higher Reynolds number this loss is negligible because the capacitor cools very quickly.

In Figure 12, the variation of heat transfer coefficient with Reynolds number and eccentricity parameter is shown. It was found that the average Nusselt number decreased as the eccentricity was increased. This trend is in good agreement with Deissler and Taylor's (12) theoretical analysis. The best line fitting the data has also been drawn in each case and it is noted that the slope of the lines is nearly constant for all eccentricities of the annulus. It was observed that the total decrease in Nusselt number was 36 per cent at the highest Reynolds number and about 40 per cent at the lowest Reynolds number. Figure 13, shows this variation at four

different Reynolds number. The rate of decrease of heat transfer coefficient was found to be greater within the first 50 per cent of the eccentricity. Between 50 and 100 per cent eccentricity the variation of heat transfer coefficient was much less.

It was pointed out in Chapter II that in the solution of equation [8] the heat transfer coefficient and the heat capacity of the test model were assumed constant. Considering the fact that the semi-log plot of equation [10] from the experimental data followed the expected straight-line relationship, these assumptions seem to be justified. A typical semi-log plot of equation [10] is shown in Figure 15. However, any definite departure from the linear relation would necessarily make the above assumptions questionable. The constancy of the heat capacity of the model will depend on the variation of the specific heat of copper with temperature. The temperature range in the present investigation was between 70 F and 140 F. It is believed that the variation of specific heat in this temperature range was negligible.

The instrument lag effect may cause an error in the measurement of heat transfer coefficient especially when the data recorded were those of a transient state. As mentioned in Chapter III, the relative error in the calculated value of the heat transfer coefficient is given by the following relation:

$$\text{Relative error} = \frac{\tau_i}{\tau_c} \times 100 \text{ per cent}$$

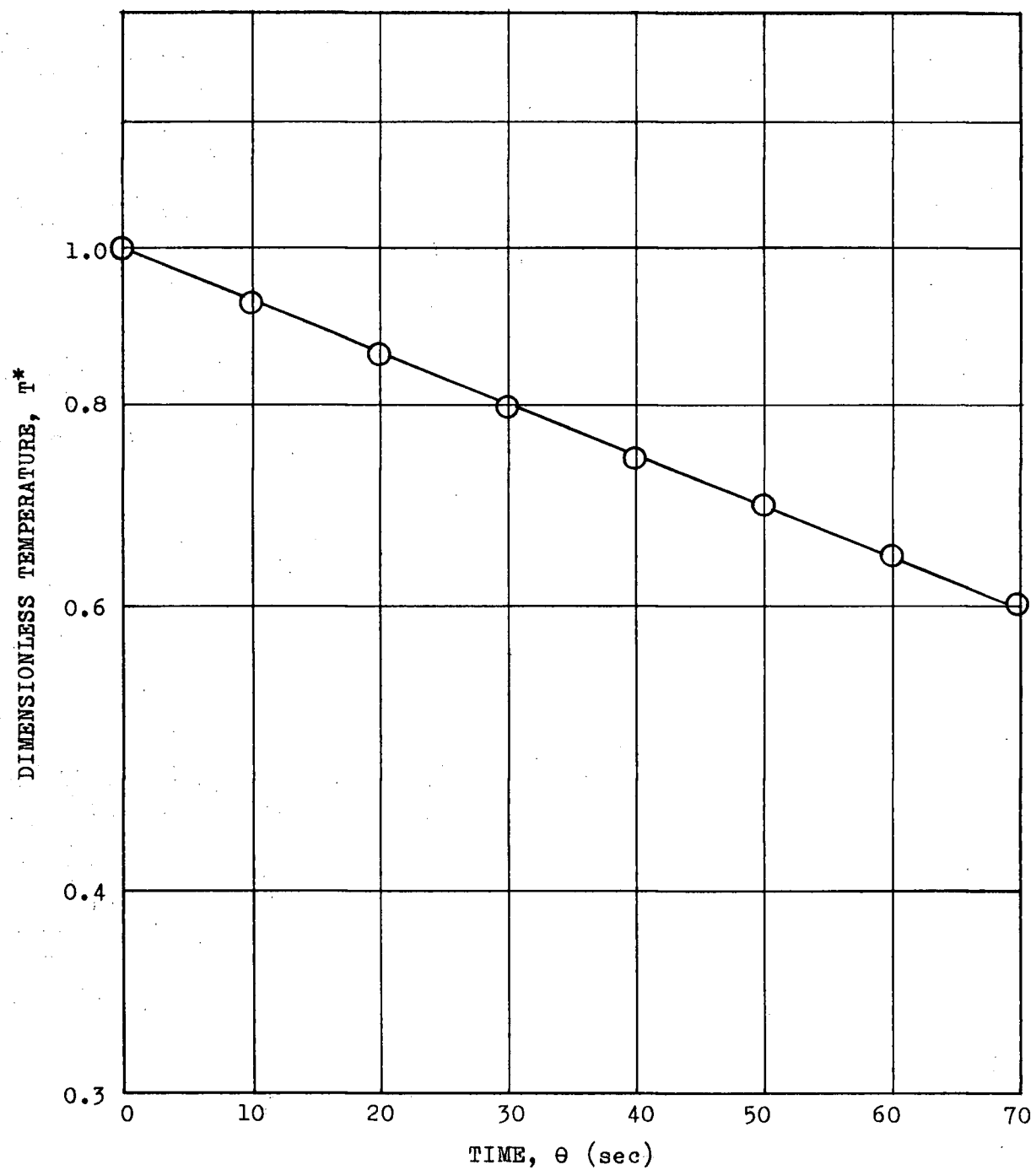


FIG. 15. TYPICAL SEMI-LOG PLOT OF DIMENSIONLESS TEMPERATURE WITH TIME

where, τ_i = time constant of the recording instrument.

τ_c = time constant of the capacitor model.

The time constant of the recording instrument was obtained by applying a step change in the input. This was found to be 2.5 sec. The time constant of the capacitor was given by the inverse of the slope of the semi-log plot shown in Figure 15. The lowest time constant of the capacitor during the entire experiment was that of Capacitor No. 1 during Run 13. This was found to be 94.5 sec. Therefore, the maximum relative error was 2.67 per cent.

In Chapter II it was assumed that the temperature gradient inside the capacitor was negligible. When the annulus was concentric this assumption was valid but one may question that this may not be the case especially when the annulus was at the maximum eccentricity, i.e., the inner tube was touching the outer tube. An experimental check was therefore made for the position $e = 1.0$ by placing the thermocouple at three different points — a, b and c shown in Figure 16 below. At one particular flow condition the maximum variation in temperature between any of the above three points was found to be less than 3 per cent.

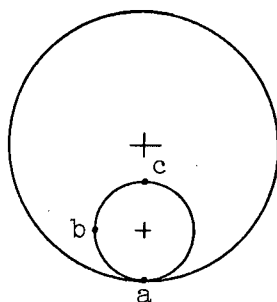


FIG. 16.

The deflection or sag of the inner cylinder could cause an error in the transient cooling of the model. When the annulus was concentric any small sag in the inner cylinder could not appreciably influence the flow pattern because of the relatively large annular thickness. Also the capacitor was mounted near the downstream support so that any small sag was around the middle of the test section which has much less influence on the capacitor. For the eccentric annulus, however, the effect of the sag of the inner cylinder could be appreciable especially at higher eccentricity. To avoid this a hollow aluminium tube was used to support the capacitor in the eccentric annulus. This is shown in Figure 2. The total deflection in the centre of the tube was, in this case, limited to 0.010 in. which is 10 per cent of the maximum annulus thickness. It was assumed that this tolerance was within the required accuracy of the experiment.

The errors due to calibration of the recording instrument and also of the thermocouples were not considered to be of any consequence. The experiment was conducted in a small temperature range and it was found that within this range the temperature-emf response of a copper-constantan thermocouple was very close to linear. Therefore, in the dimensionless temperature-time plot, Figure 15, it was sufficient to plot the logarithm of the emf ratios directly from the recorder chart. Also because of the dimensionless temperature, the calibration of the recording instrument was not required as long as it demonstrated a linear scale.

CHAPTER V

CONCLUSIONS

1. The use of the transient test technique was found to be a simple and quick method for determining the heat transfer characteristics in an annulus. Heat transfer coefficients in an eccentric annulus were found to decrease with increase in eccentricity. The decrease of heat transfer coefficient did not seem to be linearly related to the increase of eccentricity. However, the effect of eccentricity was more pronounced in the range $0 \leq e \leq 0.5$ where the value of heat transfer coefficient decreased considerably. For example, at Reynolds number of 50,000 approximately 67 per cent of the total decrease occurred in the range $0 \leq e \leq 0.5$ while the other 33 per cent occurred in the range $0.5 \leq e \leq 1.0$.

Equations of Wiegand (2) and Monrad and Pelton (3) were found to correlate the annulus data of the present investigation very well.

2. Almost isothermal data was obtained by the transient method. In the annulus, the air temperature was practically constant for one complete run and therefore the evaluation of the properties could be easily made at this temperature. This eliminates the trouble of determining the fluid film temperature required in other methods of determining the heat transfer data.

3. The temperature of the cooling capacitor was measured in an arbitrary scale during the experiment. Therefore, careful

calibration of the thermocouple and the recording instrument was not required.

RECOMMENDATION FOR FUTURE WORK

The present investigation may be considered as an exploratory work for more extensive studies in the same field. One of the important studies which is yet to be done is the behaviour of the heat transfer coefficients in the region where neither the thermal nor the hydrodynamic boundary layer has developed completely. This situation may be encountered in practice in a reactor where the heat transfer from the fuel rod is expected to take place from the very start of the tube. This investigation can probably be made by using the same technique provided a method is found to isolate the capacitors thermally along the longitudinal direction.

BIBLIOGRAPHY

- (1) London, A. L., Nottage, H. B., Boelter, L. M. K.
"Determination of Unit Conductances for Heat and Mass Transfer by the Transient Method"
Ind. and Eng. Chem.
Vol. 33, 1941, p. 467
- (2) Wiegand, J. H.
"Discussion on Annular Heat Transfer Coefficients for Turbulent Flow by McMillen and Larson"
Am. Inst. Chem. Engrs. Trans.
Vol. 41, 1945, p. 47
- (3) Monrad, C. C., Pelton, J. F.
"Heat Transfer by Convection in Annular Spaces"
Am. Inst. Chem. Engrs. Trans.
Vol. 38, 1942, p. 593
- (4) Foust, A.S., Christian, G.A.
"Non-boiling Heat Transfer in Annuli"
Am. Inst. Chem. Engrs. Trans.
Vol. 30, 1940, p. 541
- (5) Barrow, H.
"Fluid Flow and Heat Transfer in an Annulus with a Heated Core Tube"
Proc. Inst. Mech. Engrs.
Vol. 169, 1955, p. 1113
- (6) Mueller, A. C.
"Heat Transfer from Wires to Air in Parallel Flow"
Am. Inst. Chem. Engrs. Trans.
Vol. 38, 1942, p. 613
- (7) Davis, E. S.
"Heat Transfer and Pressure Drop in Annuli"
Trans. ASME
Vol. 65, 1943, p. 755
- (8) Knudsen, J. G., Katz, D. L.
"Fluid Dynamics and Heat Transfer"
McGraw-Hill Book Co. Inc.
1958
- (9) Stein, R. P., Begel, W.
"Heat Transfer to Water in Turbulent Flow in Internally Heated Annuli"
Am. Inst. Chem. Engrs. Jour.
Vol. 4, 1958, p. 127

- (10) Mizushina, T.
"Analogy between Fluid Friction and Heat Transfer in Annuli"
General Discussion on Heat Transfer - ASME/IME
1951, p. 191
- (11) Barrow, H.
"A Semi-theoretical Solution of Asymmetric Heat Transfer in Annular Flow"
Jour. Mech. Eng. Sc.
Vol. 2, 1960, P. 331
- (12) Deissler, R. G., Taylor, M. F.
"Analysis of Fully Developed Turbulent Heat Transfer and Flow in Annulus with Various Eccentricities"
NACA - TN 3451, March, 1955
- (13) Leung, E. Y., Kays, W. M., Reynolds, W. C.
"Heat Transfer with Turbulent Flow in Concentric and Eccentric Annuli with Constant and Variable Heat Flux"
NASA - N62 - 13143, August, 1962
- (14) Eber, G. R.
"Experimental Investigation of the Brake Temperature and Heat Transfer of Simple Bodies at Supersonic Speeds"
Archiv. 66/57, Peenemunde, Nov., 1941
- (15) Fischer, W. W., Norris, R. H.
"Supersonic Convective Heat Transfer Correlation from Skin Temperature Measurements on a V-2 Rocket in Flight"
Trans. ASME
Vol. 71, 1949, p. 457
- (16) Garbett, C. R.
"The Transient Method for Determining Heat Transfer Conductance from Bodies in High Velocity Fluid Flow"
Heat Transfer and Fluid Mechanics Institute
Preprints of Paper, 1951
Stanford Univ. Press
- (17) Kays, W. M., London, A. L., Lo, R. K.
"Heat Transfer and Friction Characteristics for Gas Flow Normal to Tube Banks - Use of a Transient Test Technique"
Trans. ASME
Vol. 76, 1954, p. 387

- (18) Kreith, F.
"Principles of Heat Transfer"
International Text Book Co.
1958
- (19) Miller, P., Byrnes, J. J., Benforado, D. M.
"Heat Transfer to Water in an Annulus"
Am. Inst. Chem. Engrs. Jour.
Vol. 1, 1955, p. 501
- (20) ASME Power Test Codes, Chap. 4, Part. 5
- (21) Rothfus, R. R.
"Velocity Distribution and Fluid Friction in
Concentric Annuli"
D. Sc. Thesis, Carnegie Inst. Tech.
1948
- (22) Stein, R. P., Begell, Wm.
"Heat Transfer to Water in Turbulent Flow in
Internally Heated Annuli"
Am. Inst. Chem. Engrs. Jour.
Vol. 4, 1958, p. 127
- (23) Giedt, W. H.
"Principles of Engineering Heat Transfer"
D. Van Nostrand Co. Inc.,
1958
- (24) Jordan, H.P.
"On the Rate of Heat Transmission between Fluid
and Metal Surfaces"
Proc. Inst. Mech. Engrs.
Parts 3 - 4, 1909, p. 1317
- (25) Foust, A. S., Thompson, T. J.
"Heat Transfer Coefficients in Glass Exchangers"
Am. Inst. Chem. Engrs. Trans.
Vol. 36, 1940, p. 555
- (26) Zebran, A. H.
"Clarification of Heat Transfer Characteristics
of Fluids in Annular Passages"
Ph. D. Thesis, Univ. of Michigan
1940
- (27) McMillen, E. L., Larson, R. E.
"Annular Heat Transfer Coefficients for
Turbulent Flow"
Am. Inst. Chem. Engrs. Trans.
Vol. 40, 1944, p. 177

APPENDIX I

AIR METERING SYSTEMS

The air flow rate was measured to determine the Reynolds number of the flow. The following two methods were used:

Method I. This method was used for Capacitor No. 1 at eccentricity, $e = 0$. The air flow rate was calculated based on a measurement of the maximum point velocity in the annulus. For laminar flow it has been shown that the radius at the point of maximum velocity is related to the other radii of a concentric annulus by the equation:

$$r_m = \sqrt{\frac{r_2^2 - r_1^2}{2 \log_e(r_2/r_1)}} \quad \text{-----} \quad [11]$$

Rothfus (21) has shown experimentally that the point of maximum velocity for isothermal turbulent flow of air in a concentric annulus was the same as that for laminar flow such as calculated from equation [11]. Later Knudsen and Katz (8) corroborated the same fact with their experimental results. It has also been reported by these authors that the turbulent flow velocity profile was very flat in the vicinity of the point represented by equation [11]. Knudsen and Katz gave a relation of the average to the maximum velocity as $V_{avg}/V_{max} = 0.876$ with a diameter ratio of 3.6. In the present investigation, however, the diameter ratio was 3.0. For this ratio Denton*

*Mech. Eng. Dept., Univ. of British Columbia, M.A.Sc. thesis in preparation.

studied the velocity profiles in turbulent flow and concluded that 0.876 was correct for the present annulus. The average flow velocity thus calculated had a maximum variation of 1.8 per cent.

The maximum point velocity was measured by a pitot static tube placed at the radius, r_m . It was mounted at the exit of the test section and was connected to an accurate micro-manometer capable of reading low pressures from zero in. of water head to 6.0 in. of water head.

The temperature of the air stream was measured by an ordinary mercury in glass thermometer. The thermometer was graduated to 1 F. It was found that the air temperature did not change appreciably during this part of the experiment.

The Reynolds number was finally calculated from the above data.

Method II. This method was used for the following cases:

1. Capacitor No. 1 at eccentricity, $e = 0.25, 0.5$ and 1.0 .
2. Capacitor No. 2 at eccentricity, $e = 0$.

The air flow rate was determined using a flat plate orifice mounted on a 3 in. schedule 40 pipe. Figure 3 shows the position of the orifice with respect to the test section and fan position. The orifice was designed in accordance with ASME Power Test Code (20). Straight lengths of eleven equivalent diameters at the inlet and seven equivalent diameters at the outlet of the orifice were provided as required by the code. The flow coefficient was taken from the Table given in the same reference. Table I gives the details of the orifice.

TABLE I. DETAILS OF ORIFICE

Pipe diameter, (in.)	3.068
Orifice diameter, (in.)	1.628
Flow coefficient	0.635
Pressure taps	Flange taps
Material	Stainless Steel

The orifice pressure drop and inlet side static pressure of air were measured by two ordinary U-tube manometers filled with dyed water for better visibility. The manometer scales were graduated in tenth of an inch. Since the ultimate objective was to determine the flow Reynolds number, a small error in the flow metering system was unlikely to cause any appreciable error in the final plot of the results.

Air temperature was measured by a mercury in glass thermometer graduated to 1 F.

APPENDIX II

PHYSICAL PROPERTIES AND CONSTANTS OF
THE THERMAL CAPACITORS

The dimensional details of the two thermal capacitors are shown in Figure 2. The physical properties and constants of the capacitors as required for the calculation of the heat transfer coefficients are given in the following table.

TABLE II. PROPERTIES OF THE THERMAL CAPACITORS

	Capacitor No. 1	Capacitor No. 2
Material	99.9% Copper	99.9% Copper
Length, (in.)	2.1250	1.4703
Diameter, D_1 (in.)	1.0	1.0
Mass, (gm.)	103.2312	83.8931
C_p^1 , (Btu/lb F)	0.0915	0.0915
K_s , (Btu/hr F ft)	223.0	223.0

The calculated values of Biot number based on an average heat transfer coefficient of $15 \text{ Btu/hr ft}^2 \text{ F}$ are given in the following table.

TABLE III. BIOT NUMBER OF THE CAPACITORS

	Capacitor No. 1	Capacitor No. 2
N_{Bi}	0.00583	0.00068

APPENDIX III

PHYSICAL PROPERTIES OF AIR

The properties of air required for the calculation of Reynolds and Nusselt numbers were the following:

1. Density, ρ
2. Dynamic viscosity, μ
3. Thermal conductivity, K

The density of air was determined from the equation of state. The viscosity and the thermal conductivity of air were taken from the tables given by Giedt (23). In Figures 17 and 18, these properties are shown as a function of temperature only at 14.7 lb/in² abs. pressure.

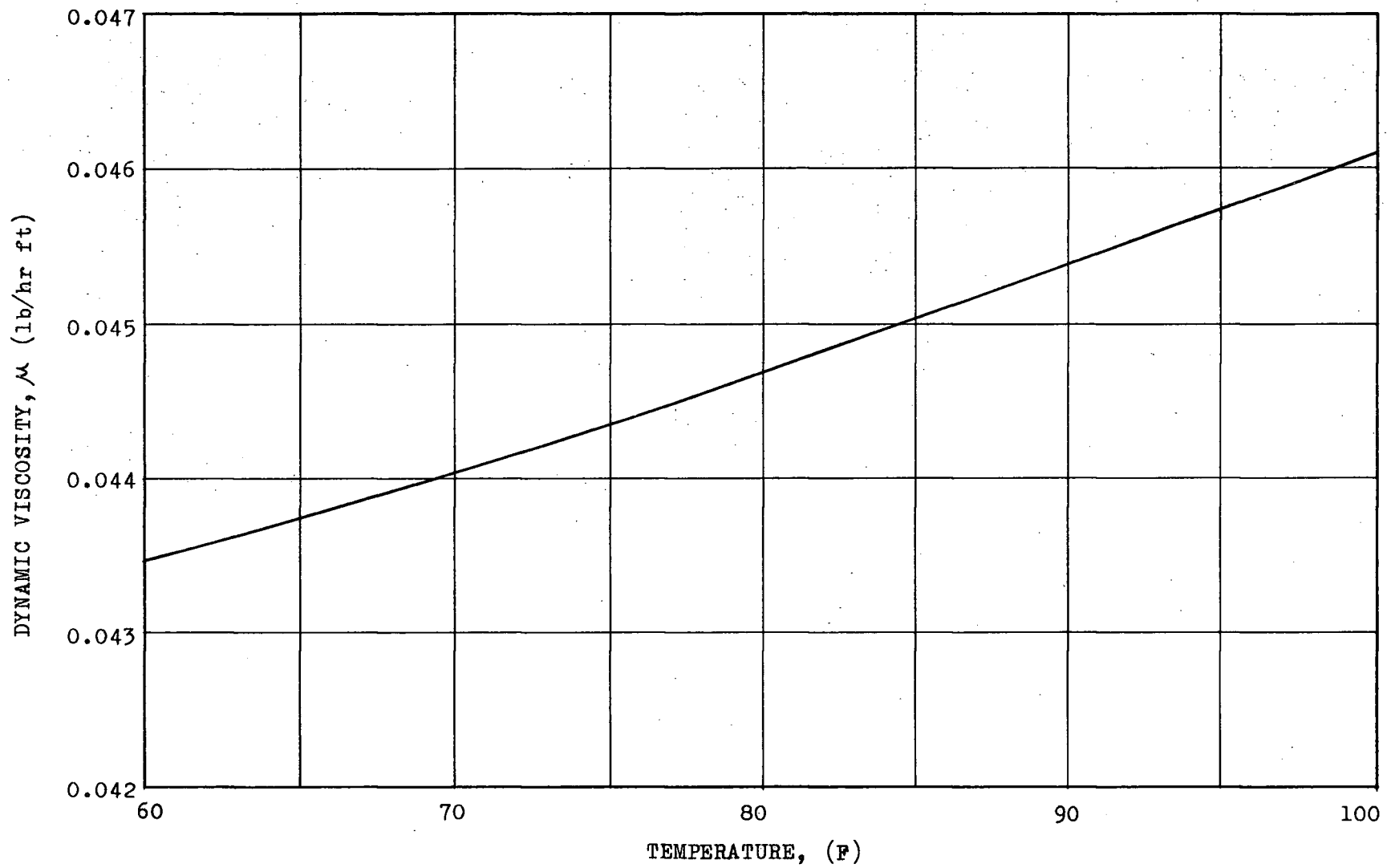


FIG. 17. DYNAMIC VISCOSITY OF AIR AT ATMOSPHERIC PRESSURE

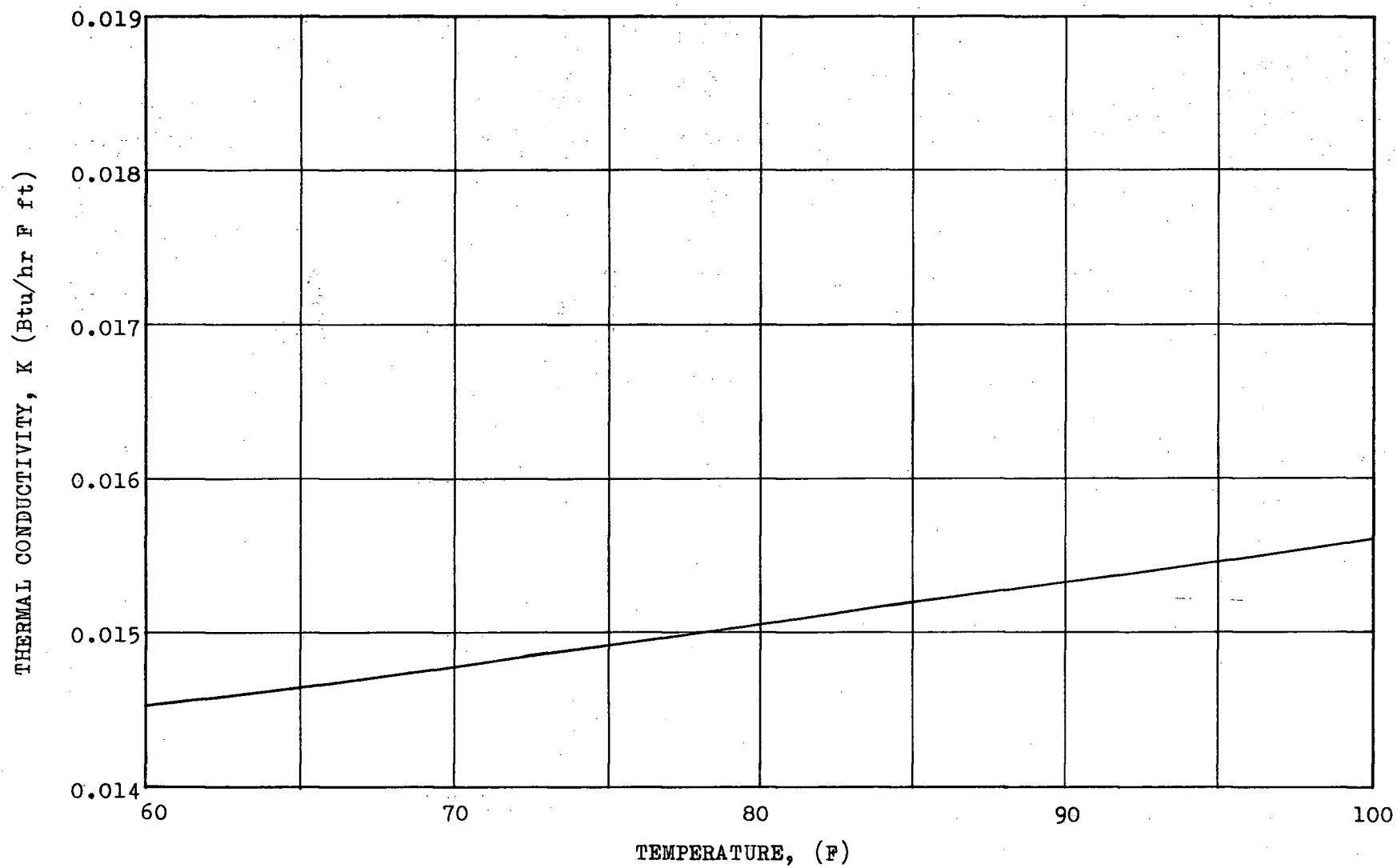


FIG. 18. THERMAL CONDUCTIVITY OF AIR AT ATMOSPHERIC PRESSURE

APPENDIX IV

SAMPLE CALCULATIONS

The following calculations of the heat transfer coefficient was done for Run 10 of the concentric annulus test. From the experimental data provided in Table IV, the values of T^* were computed which are given below.

θ (sec)	T^* (Dimensionless)
0	1.0
10	0.925
20	0.860
30	0.797
40	0.741
50	0.693
60	0.644
70	0.603

The above values are plotted in Figure 15 which gave a straight line. The slope of this line was found to be 26.2 hr^{-1} .

It was shown in Chapter II that,

Slope = $\frac{hA}{C}$. Therefore, the heat transfer coefficient was given by,

$$h = \frac{\text{Slope}}{A/C} = \frac{26.2}{2.2240} = 11.77 \text{ Btu/hr ft}^2 \text{ F.}$$

APPENDIX V

TABLES OF EXPERIMENTAL RESULTS

TABLE IV. TEMPERATURE-TIME DATA FOR CAPACITOR NO. 1, $e = 0$.
(VALUES OF T AND T_a ARE IN CHART DIV.)

Run	Time, θ (sec)								T_a
	0	10	20	30	40	50	60	70	
1	90.1	87.7	85.1	83.0	81.1	79.3	77.7	76.0	41.0
2	88.8	86.0	83.5	81.1	79.0	77.0	75.2	73.4	40.0
3	86.5	83.2	80.5	77.8	75.5	73.2	71.3	69.6	39.1
4	84.0	80.6	77.6	74.7	72.2	70.0	67.8	65.9	38.5
5	83.6	80.0	76.8	74.0	71.2	68.8	66.7	64.8	38.2
6	82.7	79.1	76.0	73.1	70.4	68.0	65.9	64.0	38.0
7	83.8	80.1	76.8	73.8	71.0	68.6	66.3	64.2	37.6
8	84.0	79.8	76.0	72.8	70.0	67.2	64.9	62.7	37.4
9	84.8	80.3	76.5	73.0	70.0	67.3	65.0	62.7	37.4
10	84.0	79.4	75.3	71.7	68.6	65.7	63.3	61.1	37.2
11	85.8	81.0	76.6	72.8	69.5	66.5	63.8	61.6	37.0
12	82.8	78.2	74.1	70.6	67.5	64.6	62.1	60.0	36.7
13	85.4	80.2	75.6	71.6	68.0	65.0	62.2	59.8	36.0

TABLE V. DATA FOR COMPUTING REYNOLDS AND NUSSELT NUMBERS
FOR CAPACITOR NO. 1, $e = 0$.

Run	T_a (F)	h_m (in water)	e (lb/ft ³)	N_{Re}	λ (1/hr)	h (Btu/hrft ² F)	N_{Nu}
1	79.0	0.08	.0747	16,700	17.6	7.91	88.0
2	78.0	0.128	.0746	21,100	19.8	8.90	99.0
3	76.5	0.195	.0746	26,100	23.5	10.55	117.3
4	76.0	0.285	.0743	31,500	26.2	11.77	131.0
5	75.7	0.335	.0745	34,200	28.0	12.58	140.0
6	75.5	0.390	.0746	36,900	28.2	12.68	141.5
7	74.8	0.450	.0745	39,600	28.6	12.85	143.5
8	74.6	0.520	.0744	42,700	31.7	14.23	159.2
9	74.6	0.565	.0744	44,500	32.6	14.65	164.0
10	74.5	0.630	.0744	46,900	35.3	15.85	177.2
11	74.0	0.705	.0744	49,700	35.8	16.09	180.0
12	73.4	0.741	.0748	51,250	35.9	16.10	180.4
13	73.0	0.818	.0747	53,750	38.1	17.10	191.8

TABLE VI. TEMPERATURE-TIME DATA FOR CAPACITOR NO. 1, $e = 0.25$
(VALUES OF T AND T_a ARE IN CHART DIV.)

Run	Time, θ (sec)								T_a
	0	10	20	30	40	50	60	70	
14	82.5	80.3	78.3	76.6	74.8	73.2	71.7	70.3	34.0
15	81.8	80.0	78.5	76.9	75.5	74.3	73.0	71.8	47.0
16	83.1	80.7	78.6	76.7	74.8	73.0	71.6	70.0	38.0
17	81.6	79.5	77.5	75.5	73.8	72.2	70.7	69.3	40.0
18	82.8	80.4	78.2	76.1	74.3	72.7	71.0	69.8	41.0
19	80.0	78.2	76.2	74.7	73.1	71.7	70.3	69.2	48.5
20	81.8	79.7	77.6	75.7	74.0	72.3	71.0	69.7	47.0
21	79.3	77.0	75.0	73.2	71.6	70.0	68.6	67.2	46.5
22	81.9	79.3	77.0	75.0	73.0	71.3	69.8	68.3	48.0
23	78.0	75.4	73.2	71.1	69.3	67.7	66.1	64.8	46.5
24	80.1	77.4	75.0	72.9	70.9	69.0	67.5	66.0	48.0
25	80.3	77.7	75.2	73.0	71.0	69.2	67.7	66.25	48.0
26	79.2	76.6	74.1	72.0	70.0	68.2	66.7	65.2	48.5
27	82.0	79.0	76.1	73.7	71.5	69.6	67.8	66.2	48.2
28	81.2	78.0	75.2	72.8	70.6	68.6	66.8	65.1	48.0
29	80.6	77.1	74.1	71.5	69.2	67.1	65.3	63.7	47.3

TABLE VII. DATA FOR COMPUTING REYNOLDS AND NUSSELT NUMBERS
FOR CAPACITOR NO. 1, $e = 0.25$

Run	T_a (F)	h_w (in.water)	h_s (in.water)	ρ (lb/ft ³)	N_{Re}	λ (1/hr)	h (Btu/hrft ² F)	N_{Nu}
14	73.5	1.35	1.1	.0747	16,430	15.00	6.73	75.4
15	85.5	1.70	1.5	.0729	17,920	17.60	7.92	86.6
16	75.5	2.10	1.8	.0743	20,400	17.90	8.06	90.0
17	78.0	2.60	2.3	.0740	22,600	18.20	8.18	91.0
18	79.0	3.20	2.8	.0742	25,050	19.82	8.92	99.0
19	87.0	3.90	3.4	.0730	27,080	21.90	9.85	107.5
20	86.0	4.90	4.3	.0735	30,550	22.32	10.05	114.6
21	85.5	6.85	6.2	.0738	36,200	23.94	10.77	118.0
22	87.0	7.90	7.0	.0737	38,800	26.50	11.92	130.2
23	85.0	9.70	8.7	.0742	43,300	28.20	12.69	139.0
24	86.5	11.30	10.1	.0746	46,750	30.10	13.54	148.2
25	86.5	12.40	11.1	.0747	49,000	29.80	13.40	146.7
26	87.0	13.40	12.0	.0747	50,800	31.60	14.21	155.2
27	86.5	14.45	12.9	.0750	53,000	32.40	14.59	159.8
28	86.0	15.65	14.1	.0751	55,200	34.30	15.42	168.6
29	85.6	16.80	15.0	.0756	57,400	36.80	16.55	181.0

TABLE VIII. TEMPERATURE-TIME DATA FOR CAPACITOR NO. 1, $e = 0.50$
(VALUES OF T AND T_a ARE IN CHART DIV.)

Run	Time, θ (sec)								T_a
	0	10	20	30	40	50	60	70	
30	86.0	84.3	82.9	81.5	80.0	78.8	77.7	76.6	47.0
31	85.0	83.1	81.5	80.0	78.5	77.1	75.9	74.8	46.0
32	86.5	84.7	82.9	81.3	80.0	78.7	77.5	76.3	48.5
33	82.2	80.5	79.0	77.6	76.1	74.8	73.7	72.6	48.6
34	82.1	80.3	78.7	77.1	75.7	74.4	73.1	72.0	49.0
35	85.0	83.0	81.2	79.5	77.8	76.5	75.2	74.0	48.0
36	80.8	79.0	77.1	75.5	74.0	72.6	71.4	70.2	48.0
37	86.1	83.6	81.4	79.5	77.5	76.0	74.4	73.0	48.5
38	80.8	78.7	76.7	74.9	73.2	71.7	70.3	68.9	47.0
39	79.8	77.3	75.2	73.3	71.6	70.0	68.6	67.3	45.0
40	83.2	80.5	78.1	76.0	74.0	72.2	70.5	69.0	48.0
41	84.4	81.7	79.2	77.0	75.0	73.3	71.7	70.2	48.5
42	79.0	76.4	74.0	72.0	70.1	68.6	67.0	65.7	47.0
43	81.2	78.2	75.2	73.0	70.8	68.8	67.2	65.7	46.0
44	81.0	77.8	74.8	72.3	70.0	67.9	66.1	64.5	45.0

TABLE IX. DATA FOR COMPUTING REYNOLDS AND NUSSELT NUMBERS
FOR CAPACITOR NO. 1, $e = 0.50$.

Run	T_a (F)	h_w (in.water)	h_s (in.water)	e (lb/ft ³)	N_{Re}	λ (1/hr)	h (Btu/hrft ² F)	N_{Nu}
30	86.2	1.5	1.25	.0728	16,580	14.17	6.37	69.5
31	86.0	2.1	1.90	.0730	19,620	15.81	7.12	76.7
32	87.0	2.5	2.20	.0730	21,700	16.20	7.30	79.6
33	88.0	3.2	2.80	.0728	24,100	17.25	7.76	84.6
34	88.0	4.0	3.60	.0728	27,000	18.95	8.52	92.9
35	87.1	4.4	3.90	.0730	28,800	19.10	8.60	93.7
36	87.0	5.5	4.90	.0734	31,800	20.2	9.08	98.25
37	86.5	6.7	6.00	.0738	35,800	22.4	10.08	110.0
38	86.0	6.8	6.00	.0737	35,600	22.4	10.08	110.3
39	84.0	8.25	7.20	.0743	39,700	23.7	10.65	117.0
40	86.0	10.0	8.80	.0740	43,150	26.7	11.0	120.2
41	86.0	11.9	10.70	.0747	48,000	26.22	11.80	129.0
42	85.0	14.0	12.30	.0750	51,400	28.9	13.00	142.3
43	84.0	16.2	14.30	.0758	56,750	30.4	13.65	150.0
44	83.0	18.15	16.05	.0758	59,900	32.25	14.50	159.5

TABLE X. TEMPERATURE-TIME DATA FOR CAPACITOR NO. 1, $e = 1.0$
(VALUES OF T AND T_a ARE IN CHART DIV.)

Run	Time, θ (sec)								T_a
	0	10	20	30	40	50	60	70.	
45	85.2	84.0	82.9	81.9	80.8	79.9	79.0	78.8	48.7
46	80.4	78.9	77.5	76.1	74.8	73.7	72.6	71.6	38.0
47	82.2	80.7	79.3	78.0	76.7	75.5	74.5	73.5	42.0
48	78.5	77.1	75.9	74.7	73.7	72.6	71.7	70.8	45.5
49	79.7	78.3	77.0	75.8	74.8	73.8	72.6	71.8	47.0
50	80.8	79.4	78.0	76.8	75.5	74.5	73.4	72.5	48.0
51	82.5	80.8	79.3	77.9	76.5	75.3	74.2	73.0	48.3
52	85.9	83.8	81.9	80.0	78.5	76.9	75.5	74.2	47.5
53	84.5	82.1	80.0	78.2	76.5	75.0	73.6	72.2	47.0
54	85.0	82.7	80.5	78.3	76.5	74.8	73.3	71.9	46.7
55	82.8	80.5	78.3	76.4	74.7	73.0	71.6	70.2	46.5
56	81.0	78.4	76.2	74.2	72.3	70.7	69.2	67.8	45.5
57	84.0	80.8	78.0	75.7	73.6	71.6	69.8	68.1	44.7
58	83.2	80.1	77.4	74.9	72.7	70.7	68.9	67.2	42.5

TABLE XI. DATA FOR COMPUTING REYNOLDS AND NUSSELT NUMBERS
FOR CAPACITOR NO. 1, $e = 1.0$.

Run	T_a (F)	h_w (in.water)	h_s (in.water)	ρ (lb/ft ³)	N_{Re}	λ (1/hr)	h (Btu/hrft ² F)	N_{Nu}
45	88.0	1.3	1.1	.0725	15,600	11.49	5.17	56.25
46	76.0	1.3	1.2	.0743	16,070	12.25	5.51	61.50
47	79.0	1.9	1.1	.0738	19,300	12.80	5.75	63.80
48	84.0	2.4	2.2	.0734	21,450	14.13	6.35	69.70
49	85.0	3.2	2.8	.0733	24,600	15.35	6.90	75.60
50	87.0	3.7	3.2	.0730	26,350	15.45	6.95	76.00
51	87.0	4.7	4.1	.0730	29,700	16.90	7.60	83.00
52	86.0	6.2	5.3	.0736	34,400	19.26	8.66	94.50
53	86.5	8.4	7.2	.0740	40,200	20.00	9.00	98.40
54	85.0	10.2	8.8	.0742	44,300	22.10	9.94	108.90
55	85.0	11.8	10.2	.0747	47,800	22.15	9.95	109.00
56	83.5	13.6	11.7	.0750	51,600	24.60	11.05	121.50
57	82.0	16.05	13.8	.0755	56,200	26.22	11.80	130.00
58	80.0	18.35	15.9	.0764	65,000	26.30	11.80	130.50

TABLE XII. TEMPERATURE-TIME DATA FOR CAPACITOR NO. 2, $e = 0$
 (VALUES OF T AND T_a ARE IN CHART DIV.)

Run	Time, θ (sec)								T_a
	0	10	20	30	40	50	60	70	
59	86.6	85.0	83.5	82.0	80.7	79.3	78.2	77.0	47.0
60	79.7	78.0	76.5	75.2	74.0	72.8	71.7	70.6	47.5
61	80.0	77.9	76.1	74.5	73.0	71.6	70.2	69.0	46.7
62	79.8	77.5	75.4	73.6	71.8	70.2	68.9	67.5	46.0
63	81.0	78.0	75.5	73.3	71.2	69.5	67.7	66.3	45.0
64	79.7	76.7	73.8	71.5	69.3	67.4	65.7	64.2	44.0
65	80.2	76.5	73.3	70.4	67.9	65.7	63.7	62.0	43.0

TABLE XIII. DATA FOR COMPUTING REYNOLDS AND NUSSELT NUMBERS
FOR CAPACITOR NO. 2, $e = 0$

Run	T_a (F)	h_w (in.water)	h_s (in.water)	ρ (lb/ft ³)	N_{Re}	λ (1/hr)	h (Btu/hrft ² F)	N_{Nu}
59	86.0	1.25	1.1	.073	15,400	14.35	7.57	83.0
60	86.0	2.90	2.5	.0732	23,420	17.10	9.03	99.0
61	85.0	4.70	4.0	.0735	29,900	21.10	11.15	122.0
62	84.5	7.05	6.1	.0740	36,900	23.35	12.32	135.0
63	83.0	10.4	9.0	.0747	45,000	27.30	14.40	158.4
64	82.0	13.2	11.4	.0752	51,000	30.30	16.00	176.2
65	80.5	18.35	16.0	.0745	59,900	34.60	18.28	202.0